International Journal for Computational Civil and Structural Engineering, 21(1) 157–188 (2025)

DOI:10.22337/2587-9618-2025-21-1-157-188

CREEP EFFECT ON BEHAVIOR OF ECCENTRICALLY LOADED REINFORCED CONCRETE COLUMNS MADE OF HIGH-STRENGTH CONCRETE

Dmitry A. Strakhov, Aleksey O. Baranov

Peter the Great St. Petersburg Polytechnic University, St. Petersburg, RUSSIA

Abstract: The focus of the research is on eccentrically loaded reinforced concrete elements made of high-strength concrete with mineral additives such as fly ash and silica fume. The behavior of eccentrically loaded reinforced concrete elements was studied on a reinforced concrete column. At the age of 90 days the reinforced concrete column was subjected to a compressive force of 66 kN with an eccentricity of 12.5 cm. The loading duration was 245 days. During the tests, the average strains caused by eccentric loading, shrinkage, and creep concrete on the column were measured. In addition, the deflections and crack opening widths were measured. Experimental data were compared to theoretical data obtained using a stepwise version of the elastic solutions method (the stepwise method). In this method, the continuous change of stresses and strains of reinforced concrete elements under loading is replaced with a stepwise change. The considered loading time is divided into specific intervals (steps). Due to the creep of concrete, the conditions for compatibility of deformations are violated at the end of each step. The restoration of the conditions is carried out due to elastic deformations while simultaneously satisfying the conditions of static equivalence. The results of the comparison demonstrate that the stepwise meth-od adequately describes the changes of strains and deflections of eccentrically loaded reinforced concrete columns made from high-strength concrete over time. For the first time, the stepwise method was used to calculate the crack opening width. The calculation results are in good agreement with the experiments and show a significantly smaller increase in crack opening over time compared to that calculated according to Russian Building Codes.

Keywords: high-strength concrete, fly ash, silica fume, reinforced concrete, creep, eccentric loading, deflection, strain

НАПРЯЖЕННО-ДЕФОРМИРОВАННОЕ СОСТОЯНИЕ ВНЕЦЕНТРЕННО СЖАТЫХ ЭЛЕМЕНТОВ ИЗ ВЫСОКОПРОЧНОГО БЕТОНА ПРИ ДЛИТЕЛЬНОМ НАГРУЖЕНИИ

Д.А. Страхов, А.О. Барано[1]

Санкт-Петербургский политехнический университет Петра Великого, г. Санкт-Петербург, РОССИЯ

Аннотация: Объектом исследования в данной работе являются железобетонные внецентренно сжатые элементы из высокопрочного бетона с использованием минеральных добавок (зола уноса, микрокремнезем). Исследование напряжено-деформированного состояния внецентренно сжатых элементов выполнялось на примере железобетонной колонны. Колонна в возрасте бетона 90 суток подвергалась длительному нагружению в пружинной установке сжимающей силой, равной 66 кН, с эксцентриситетом 12.5 см. Продолжительность нагружения составила 245 суток. В период выдерживания под нагрузкой измерялись средние деформации в сжатой зоне, средние деформации сжатой и растянутой арматур, перемещения (прогибы) и ширина раскрытия трещин. Опытные данные сопоставлялись с теоретическими, полученными в соответствии с шаговым вариантом метода упругих решений (метод ступенек). В этом методе непрерывное изменение напряжений и деформаций в железобетонных элементах под нагрузкой заменяется на ступенчатое изменение. Весь исследуемый период времени разбивается на отдельные интервалы (шаги). В конце каждого интервала условия совместности деформаций нарушаются из-за ползучести бетона. Восстановление условий осуществляется за счет упругих деформаций при выполнении условий статического равновесия.

Результаты сравнения показали, что рассмотренный метод удовлетворительно описывает изменения деформаций и прогибов внецентренно сжатых колонн из высокопрочного бетона при длительном нагружении. Кроме того, впервые шаговый вариант метода упругих решений использовался для вычисления ширины раскрытия трещин.

Ключевые слова: высокопрочный бетон, зола уноса, микрокремнезем, железобетон, ползучесть, внецентренно сжатые элементы, прогибы, деформации

INTRODUCTION

The creep of high-strength concrete is of particular importance in the design of reinforced concrete structures of high-rise buildings [1,2]. The use of high-strength concrete allows for the creation of structural elements with smaller cross-sectional areas. This has a positive economic impact as it reduces the amount of material required to construct a structure and increases the usable space within the building. However, this leads to a reduction in their rigidity and an increase in the deflection. This trend is particularly noticeable during prolonged loading, when creep deformation occurs, which has not yet been fully studied for high-strength concrete.

It is known that the addition of mineral additives to concrete, such as fly ash [3–5], silica fume [6–8], ground granulated blast furnace slag [9,10], metakaolin [11,12], can reduce creep. However, a different outcome was achieved in the studies [7,13,14].

The article [7] reported that replacing 10% of the cement with silica fume (SF) increased the creep of concrete during the early stages of loading (0 to 60 days) compared to a control mixture (without silica fume). However, after 60 days of loading, the rate of creep deformation decreased, and after 360 days, the creep deformation of concrete with 10% SF was approximately 85% that of concrete without added SF.

In [14], creep deformation after 150 days of observation was 16%, 33%, and 55% higher for concrete mixes containing 20%, 40%, and 60% ground granulated blast furnace slag (GGBFS) respectively, compared to the control mix without slag. In the study [13], the deflections of reinforced concrete beams in the middle part of the span caused by concrete creep were 30%, 70%, and 100% higher for concrete mixes containing 20%, 40%, and 60% GGBFS, respectively, compared to beams made from control concrete mixes, after 150 days of observation. The values of the long-term load during the tests were 25% of the load values at the time of crack formation.

Steel and basalt fibers can reduce creep strains in concrete, both under compressive and tensile loads [15–17]. Reinforcing fibers with a low modulus of elasticity, such as polypropylene fibers or polyvinyl alcohol fibers, can increase creep in concrete [18,19].

The use of aggregates made from recycled materials [20–22] and industrial waste [23,24] as a substitute for natural aggregates increases the creep of concrete.

In work [25], short reinforced concrete columns were loaded with a long axial load. The creep coefficient of reinforced concrete columns decreased as the compressive strength of concrete and the reinforcement ratio increased. An expression is proposed to account for the effect of longitudinal reinforcement on the creep of concrete in reinforced concrete columns. In articles [26,27], it is noted that longitudinal reinforcement has a retarding effect on the creep of concrete.

In the study [28], reinforced concrete cantilever columns were subjected to long-term loading with a force applied at an eccentricity. Axial shortening and deflection increase over time due to creep and shrinkage of concrete. However, this increase decreased rapidly as time increased. Axial shortening and deflection of eccentrically loaded cantilever columns in experiments agreed well with the predictions based on existing models for concrete creep and shrinkage, as proposed in ACI 209R-92 [29].

In the article [30], the experimental values of the specific creep of high-strength concrete

were compared with the calculated values obtained using different theoretical models. The CEB-FIP [31], GL2000 [32], B4 [33], and ACI 209 [29] models significantly overestimate the specific creep strains compared to the experimental values. The B4 model satisfactorily predicts the creep of high-strength concrete. The articles [34,35] note that existing models for predicting creep in conventional concrete cannot be applied to high-strength concrete.

The analytical model presented in the article [36] takes into account the effects of creep, geometric nonlinearity, cracking, shrinkage, and aging in concrete. Numerical research has shown that creep in reinforced concrete columns leads to an increase in internal forces and deflections over time. The article [37] presents a new approach to calculating the behavior of reinforced concrete shells. The method is based on replacing the actual shell with an equivalent elastic shell.

In [38], reinforced concrete beams made from high-strength concrete were tested for pure bending. The experimental values of the destructive load were slightly higher than predicted by the calculations. Studies [39,40] contain the results of experimental studies of high-strength fiber reinforced concrete beams with round cross-sections under combined bending and torsion. Article [41] proposes expressions that make it possible to consider force and temperature effects jointly in calculations of reinforced concrete bending elements.

The article [42] compares the experimental data on strains and deflections of a reinforced concrete beam made of ordinary concrete under prolonged loading with calculated data obtained using the stepwise elastic solution method (the stepwise method). The results of the comparison showed good agreement.

The creep of high-strength concrete has not yet been fully studied. Additionally, the behavior of different types of reinforced concrete structures made from high-strength concrete under prolonged loads has not been adequately studied. The above-mentioned stepwise method can quite accurately describe the behavior of most types of rods reinforced concrete structures made of ordinary concrete. However, no studies have compared the calculated values with experimental data of reinforced concrete elements made from high-strength concrete under prolonged loading. Therefore, this study aimed to investigate the behavior of eccentrically loaded reinforced concrete elements made of high-strength concrete under prolonged loading and to compare experimental data with theoretical data obtained using a stepwise version of the elastic solutions method.

METHODS AND MATERIALS

Experimental research

The study of the behavior of eccentrically loaded compressed elements was conducted on a reinforced concrete column made from high-strength concrete with a cross-section of 15 x 10 cm and a height of 120 cm.

The following materials, with their respective characteristics, were used to create high-strength concrete: Portland cement CEM I 42.5 N from JSC "CEMROS" from the Peterburgcement plant in St. Petersburg, Russia; natural sand with a SiO_2 content of at least 81.4% and a fineness modulus of 2.3 produced by the "REMIKS" company in St. Petersburg, Russia; granite crushed stone (fractions from 5-10 mm and 10-20 mm), JSC "Semiozerskoe kar'eroupravlenie", quarry "Perovskij", Leningrad region, Russia; tap water; modifier for concrete "MB10-30S A I-2", LC "Predprijatie Master Beton", Moscow, Russia.

The modifier "MB10-30S A I-2" [43] was added to the concrete mix in an amount of 20% of the cement weight. The modifier contains the indicated ingredients in the following quantities (in % of total weight): silica fume 63%, fly ash 27%, and superplasticizer based on naphthalene-formaldehyde polycondensation 10%.

Table 1. Chemical composition of modifier "MB10-30S A I-2" and Portland cement CEM I 42.5N

Chemical composition by weight, %	Materials	
	Modifier	Cement
SiO_2	70.8	21.2
Al_2O_3	12.2	4.6
Fe_2O_3	2.1	4.2
CaO	0.7	62.9
MgO	0.6	1.7
SO_3	0.5	2.8
K_2O	0.6	0.6
Na_2O	0.4	0.3

Table 2. Mix proportions of concrete (kg/m³)

Ingredient	Proportions
Cement	490
Sand	790
Crushed stone	850
Water	170
Modifier	100
W/C	0.35
Density of compacted fresh concrete, kg/m³	2367

The modifier is a gray powdered material with a bulk density of 776 kg/m³. Table 1 shows the chemical composition of the modifier "MB10-30S A I-2" and Portland cement CEM I 42.5N. Table 2 provides basic information on the composition of high strength concrete.

The concrete mixture was poured into the moulds in a horizontal position. After that, it was compacted by tamping and vibration on a laboratory vibration table, model C279, manufactured by "Matest" in Italy (**Ошибка! Источник ссылки не найден.**). The specimens were kept in moulds for 24 hours at room temperature 20 ± 5°C. Afterward, they were demoulded and placed in a standard curing room with a controlled temperature of 20 ± 2°C and relative humidity of more than 95%. After 27 days, the specimens were removed from the standard curing room and stored in laboratory conditions at a temperature of 20 ± 2 ° C and an air humidity of 60 ± 5% until testing.

Figure 1. Production of concrete mix

The concrete mixture was prepared in a forced concrete mixer, model C162, manufactured by "Matest" in Italy (Fig. 1). The workability of the concrete mixture was determined using a concrete slump test in accordance with the Russian State Standard GOST 10181-2014 [44]. The slump of fresh concrete cone was 18 cm.

Figure 2. Compacting fresh concrete with tamper and vibration on laboratory vibrating table

Table 3. Mechanical properties of high-strength concrete at age 28 and 90 days

Mechanical properties	Age of concrete	
	28 days	90 days
Compressive strength, MPa	90.4	93.6
Splitting tensile strength, MPa	3.26	3.90
Prismatic compressive strength, MPa	68.2	70.5
Modulus of elasticity, GPa	36.5	38.3

Table 3 shows the mechanical properties of high-strength concrete at 28 and 90 days, as determined according to the Russian State Standards GOST 10180-2012 [45] and GOST 24452-80 [46]. The compressive strength and splitting tensile strength of concrete were determined on cubes with a side length of 10 cm. The values of strength obtained in tests were multiplied by coefficients of 0.95 and 0.88 respectively to calculate the compressive and splitting tensile strengths of concrete for cubes with a basic dimension of 15 cm in accordance with the Russian State Standard GOST 10180-2012 [45]. The prismatic compressive strength and modulus elasticity of concrete were determined on prism specimens with dimensions of 10x10x40 cm.

The characteristics of the mechanical properties of high-strength concrete were used as initial data to calculate the behavior of an eccentrically loaded reinforced concrete column using a stepwise version of the elastic solutions method.

Laminated plywood with a thickness of 18 mm was used to create the formwork for the reinforced concrete column. The formwork was previously lubricated with engine oil. Fig. 3 shows a general view of the formwork and reinforcement frame. There were two bars of tensile reinforcement with a diameter of 12 mm and two bars of compressed reinforcement installed with 6 mm in the column. The class of longitudinal steel reinforcement bars was A400, with a yield strength of 400 MPa. Steel bars with a diameter of 6 mm and class A 240 with a yield strength of 240 MPa were used as transverse reinforcement. The reinforcement bars in the frame were joined by welding.

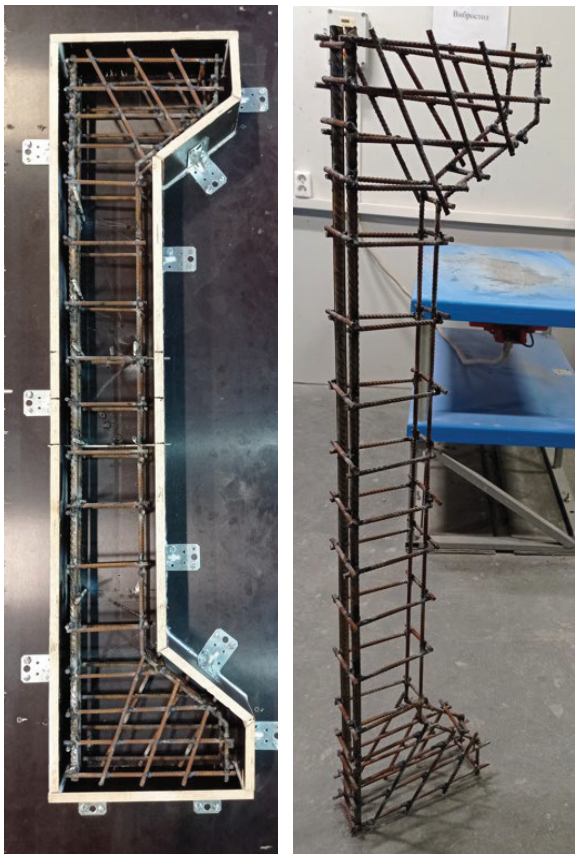

Figure 3. General view of formwork, reinforcement frame

After 24 hours of production, the column was removed from the formwork. Then it was placed in laboratory conditions with a temperature of 20 ± 5 °C and an air humidity of 60 ± 5% until testing.

Fig. 4 shows a general view of the reinforced concrete column in the testing setup. The age of the concrete at the time of testing was 90 days. A compressive force (P) of 66 kN was applied with an eccentricity (e) of 12.5 cm from the longitudinal axis of the element, as shown in Fig. 5. A hydraulic jack (LLC "Belak-Rus", in Russia) with a capacity of 50 tons was used to apply a compressive force to the column. The load on the column was applied in steps of 15% of the total load value (66 kN) during testing. At each stage, the load was maintained for 10 minutes.

Figure 4. General view of reinforced concrete column and testing setup

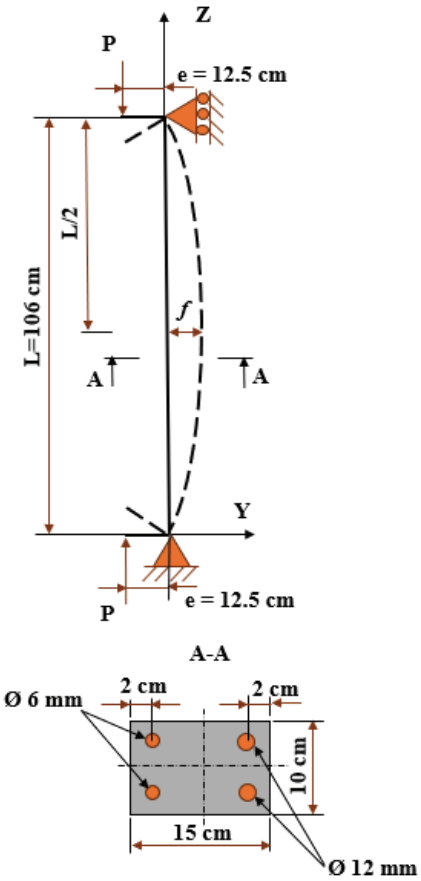

Figure 5. Testing scheme

The strains were measured in the middle of the column using dial indicators with a graduation of 0.001 mm (produced by "Micron" in the Czech Republic). The strains of the extreme fiber in the compression zone and the compressed reinforcement were measured using a base length of 15 cm. The strains of tensile reinforcement were measured using a base length of 35 cm.

The deflections of the reinforced concrete column were measured in the middle of the height using dial indicators with a graduation of 0.01 mm (produced by "Micron" in the Czech Republic). In addition, dial indicators were installed at the intended support points (70 mm from the column ends) to monitor possible movements of the test setup.

The width of the crack of the reinforced concrete column was measured using a microscope with the price of division of 0.02 mm.

Numerical method

To compare the experimental results with the calculated ones, a stepwise version of the method of elastic solutions was used, which is based on the following principles:

– the distribution of concrete and reinforcement strain along the depth of the element section is assumed according to a linear law (hypothesis of plain sections);

– the resistance of concrete in the tensile zone is not taken into account; all tensile force is taken by the reinforcement;

– the relationship between stresses and instantaneous strains is linear, i.e., stresses under instantaneous loading are determined as for an elastic body;

– increments of creep strain (over a short time interval) are determined without considering the change in stress over the same interval.

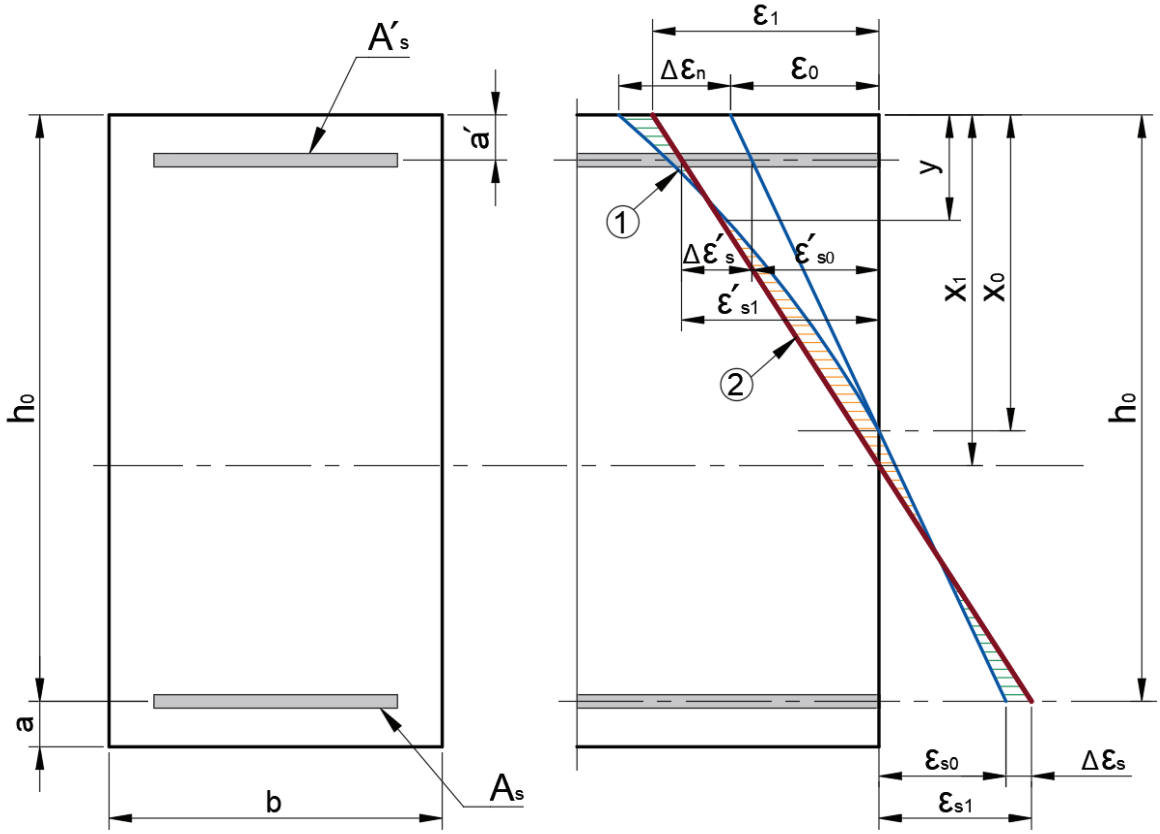

Figure 6. Transformation scheme ensuring implementation of condition of compatibility of deformations (hypothesis of plane sections)

The stepwise version of the method of elastic solutions (stepwise method) allows one to quite accurately take into consideration the main features of the strains of reinforced concrete elements under long-term load action [42]. The ability to consider the actual duration of each load component is a significant advantage of this method both when analyzing the stress-strain state and when calculating displacements (deflections) and crack opening width.

Calculation of the behavior using the stepwise method is carried out as follows.

1. The continuous change in stress and strain is replaced by a step change. The entire time period under study is divided into intervals Δt, that are quite small and not necessarily equal in size.

2. At the beginning of the first interval, stress and strain are determined by solving the corresponding elastic problem. The resistance of tensile concrete is not considered.

3. Creep strains during the interval are determined under the assumption of constant stresses during this interval.

4. Due to creep, the conditions for compatibility of deformations are violated. They can be satisfied only through instantaneous strains, for which it is necessary to apply such a stress state that would restore the conditions of compatibility while simultaneously satisfying the conditions of static equivalence.

Next, the following time interval is considered, taking into account stress changes during the previous interval.

For a reinforced element of arbitrary cross-section with a double reinforcement, the transformation that ensures the fulfillment of the condition of compatibility of deformations is presented in the diagram below (see Fig. 6).

During the interval Δt, creep strain develops. At each point of the compressed zone at the end of the interval, the strain is expressed

$$\varepsilon(y) = \varepsilon_0(y) + \Delta\varepsilon_n(y), \tag{1}$$

where y is the distance from the compressed edge of the section to the point in question; $\varepsilon(y)$ is the total strain at a point with a coordinate y until the condition of compatibility of strains is satisfied.

A total strain diagram is formed at the end of the interval, indicated by the number 1 (Fig. 6), which does not satisfy the condition of compatibility of deformations. The purpose of the transformation is to find a strain diagram (indicated by number 2 in Fig. 6) that would satisfy the compatibility condition (the hypothesis of plane sections), as well as the equilibrium conditions.

When implementing the stepwise method, the following notations are adopted: x_0 is the height of the compressed zone at the beginning of the interval Δt; x_1 is the depth of the compressed zone at the end of the interval after the transformation has been carried out; ε_0 is the shortening deformation in the upper fiber of the section at the beginning of the interval (at the beginning of the first interval it is elastic strain, while at the beginning of subsequent intervals it contains both elastic and creep strain); $\Delta\varepsilon_n$ is the increment of creep strain in the top fiber of the section during the interval Δt; ε_1 is the shortening deformation in the upper fiber of the section at the end of the interval Δt after the transformation has been carried out; ε_{s0} and ε'_{s0} are the strains of tensile and compressed reinforcement at the beginning of the interval Δt; $\Delta\varepsilon_{s0}$ and $\Delta\varepsilon'_{s0}$ is the increment in strains of tensile and compressed reinforcement during the interval; ε_{s1} and ε'_{s1} are the strains of tensile and compressed reinforcement at the end of the interval after the transformation.

To solve the problem, it is necessary to determine the following quantities $x_1, \varepsilon_1, \varepsilon_{s1}$ and ε'_{s1}. The first two can be found from two static equations, and the last two can be expressed through and from the condition of compatibility of deformations. Using the latter, we get:

$$\varepsilon_{s1} = \frac{\varepsilon_1(h_0 - x_1)}{x_1}; \tag{2}$$

$$\varepsilon'_{s1} = \frac{\varepsilon_1(x_1 - a')}{x_1}. \tag{3}$$

The equality to zero of the projections of the stress increments sum on the horizontal axis gives

$$\begin{aligned} &E_b\int_0^{x_1}\frac{\varepsilon_1(x_1-y)}{x_1}b(y)dy - \\ &-E_b\int_0^{x_0}\varepsilon(y)b(y)dy - E_b n A_s\Delta\varepsilon_s + \\ &+E_b n A'_s\Delta\varepsilon'_s = 0\ , \end{aligned} \tag{4}$$

where $n = \frac{E_s}{E_b}$,

E_b is the initial modulus of elasticity of concrete (under instantaneous loading);

E_s is the modulus of elasticity of the reinforcement.

Using the equality to zero of a sum of the static moments of stress increments relative to the axis of the tensile reinforcement, we have

$$\begin{aligned} &E_b\int_0^{x_1}\frac{\varepsilon_1(x_1-y)}{x_1}(h_0-y)b(y)dy - \\ &-E_b\int_0^{x_0}\varepsilon(y)(h_0-y)b(y)dy + \\ &+E_b n A'_s\Delta\varepsilon'_s(h_0-a') = 0. \end{aligned} \tag{5}$$

The universal form of writing equations (4) and (5) allows us to have the same forms for bending, eccentric compression, and eccentric tension.

Having determined the values of x_1 and ε_1, the stresses at any point in the compressed zone at the end of the interval can be obtained using the formula

$$\sigma(y,t) = \overline{\sigma}(y,t) + \\ + E_b\left[-\varepsilon(y,t) + \frac{\varepsilon_1(x_1 - y)}{x_1}\right], \quad (6)$$

where $\overline{\sigma}(y,t)$ are the stresses at the beginning of the interval; $\varepsilon(y,t)$ are total strain at the end of the interval before transformation.

Stresses in the tensile and compressed reinforcement in a section with a crack at the end of the interval are determined using the formulas:

$$\sigma_s = \varepsilon_{s1} E_b n; \quad (7)$$

$$\sigma'_s = \varepsilon'_{s1} E_b n. \quad (8)$$

With a time-varying external load, within the framework of this method, the continuous load change should be replaced by a step change, and individual steps should be applied "instantaneously" at the boundaries of time intervals. In this case, the resulting strains must satisfy the law of linear distribution over the depth of the section, and the stress state must satisfy the equilibrium conditions. The implementation of these conditions leads to the fact that with an instantaneous increase in load, the depth of the compressed zone decreases, and the neutral axis in terms of stress is located closer to the compressed face of the element than the neutral axis in terms of total strain. With an instantaneous decrease in load, the depth of the compressed zone of the section increases, and the neutral axes in terms of stress and total strain coincide.

The element deflections due to the total strains (instantaneous and creep strains) at the end of each time interval can be determined using the Mohr integral according to the formula

$$f = \sum_{j=1}^{n} \int_{a_j}^{b_j} \omega_j(t) \bar{M}_j dx, \quad (9)$$

where n is the number of integration sections along the length of the element; j is the integration section number; $\omega_j(t)$ is the average curvature of the axis of the corresponding section of the element; $\bar{M}_j$ is the bending moment in the section with the index j from a unit force applied at the point and in the direction of the determined displacement.

In accordance with the considered calculation method, at the end of each time interval, the total strains of the extreme compressed concrete fiber and tensile reinforcement) in the section with a crack are known. In calculations, cross sections in the middle of each section along the length should be considered; the corresponding curvatures can be calculated using the formula

$$\omega_j(t) = \frac{\varepsilon_{bj}\psi_b + \varepsilon_{sj}\psi_{sj}}{h_0}, \quad (10)$$

where ψ_b and ψ_{sj} are the coefficients of transition from strains in the section with a crack to average strains in the area between the cracks.

The coefficient ψ_b can be taken as equal to 0.9. The coefficient ψ_{sj} is calculated using the formula

$$\psi_{sj} = 1 - 0.8\frac{\sigma_{s,crc(j)}}{\sigma_{s(j)}}, \quad (11)$$

where $\sigma_{s,crc(j)}$ is the stress in the longitudinal tensile reinforcement in the section with a crack immediately after the formation of normal cracks for the section with index j.

The stress $\sigma_{s,crc(j)}$ can be determined by using a first approximation under instantaneous loading (without taking creep into account), and the values in accordance with the considered step method are known at the end of each time interval.

The crack opening a_{crc} in the calculations below was determined in accordance with the methodology adopted in the current standards, with the exception of the strains of the tensile reinforcement and the area of the tensile zone of concrete, which are known directly from the calculation using the step method, and the duration coefficient for prolonged action of the load, since its actual duration was taken into consideration in the calculations.

RESULTS AND DISCUSSION

Fig. 7 shows the experimental data of the average concrete strains in the compressed zone and the average strains of tensile and compressive reinforcement in a reinforced concrete column. By average, we mean strains averaged over the length of the indicator base, including strains in cross sections with cracks. In addition, the strains obtained in the experiment are complete, i.e., elastic strains and strains caused by creep and shrinkage of concrete.

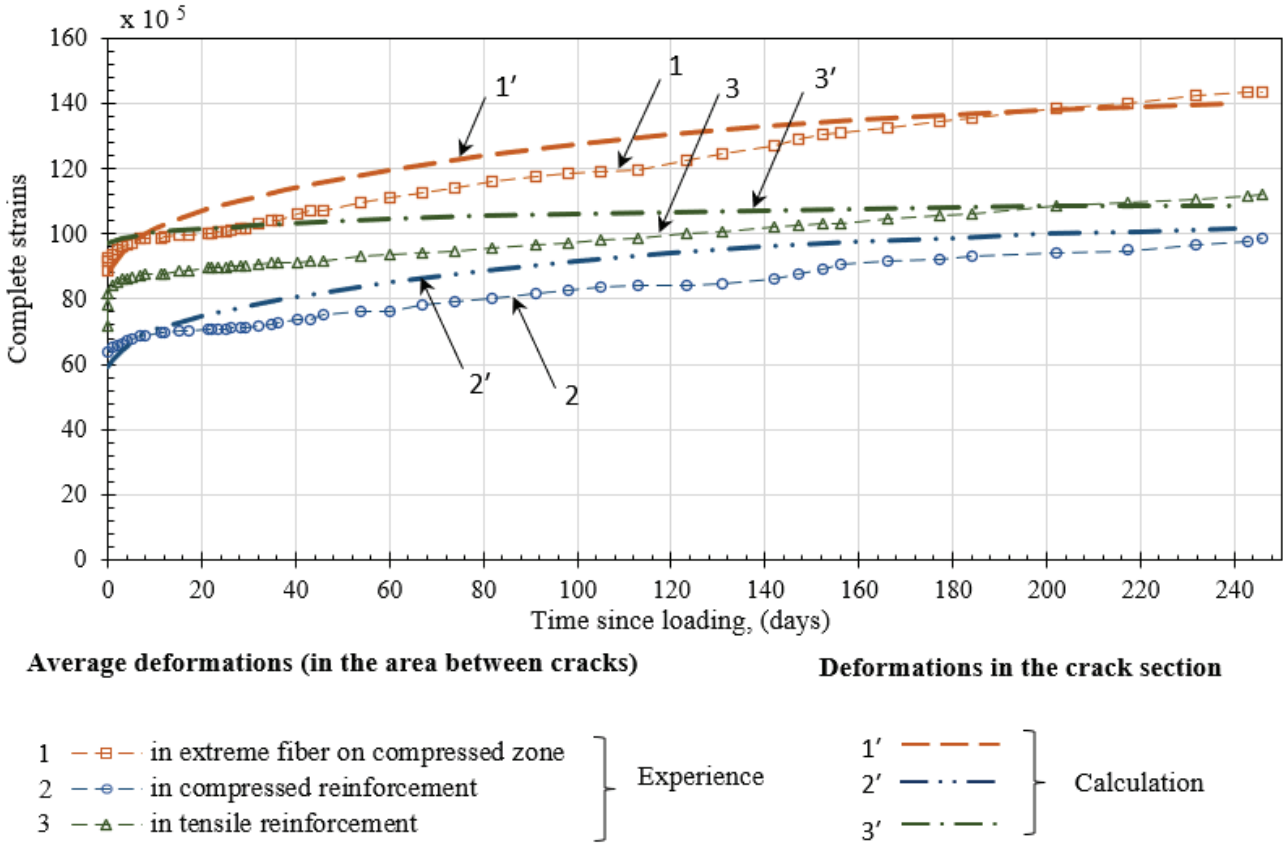

Figure 7. Comparison of experimental average strains and calculated strains in section with crack (using the stepwise method) for reinforced concrete column made of high-strength concrete

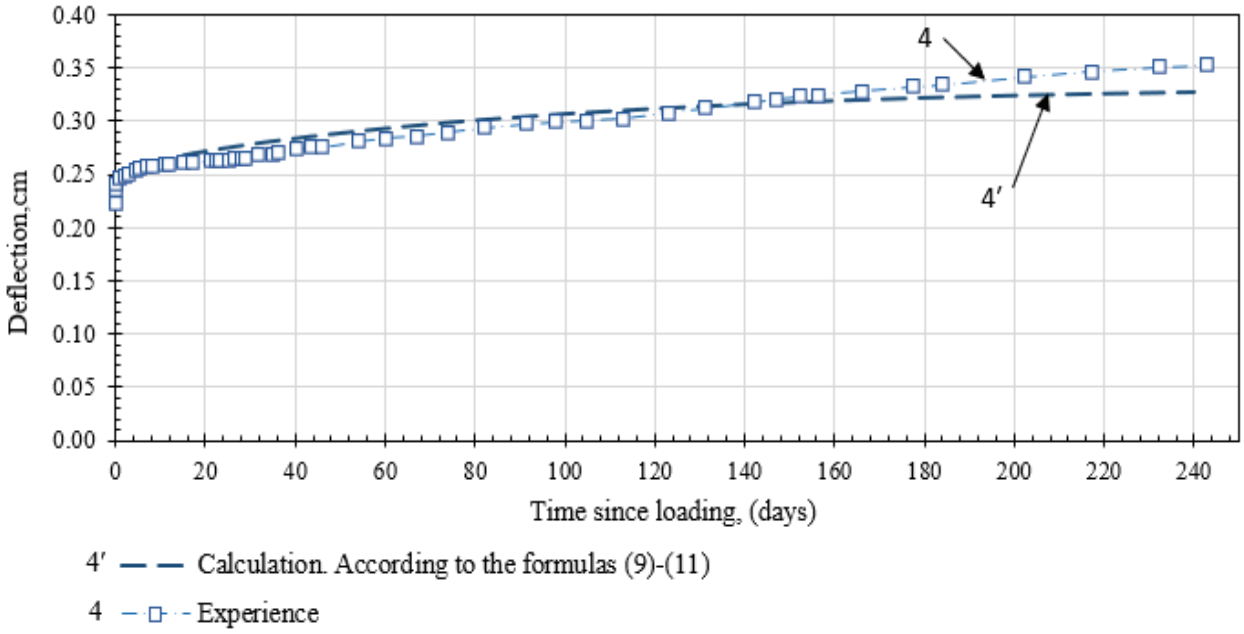

Figure 8. Comparison of experimental and calculated values of deflections in middle part of height of reinforced concrete column made of high strength concrete

It should be noted that Fig. 7 shows experimental strain values of compressed and tensile reinforcement according to direct readings of dial indicators installed on the side faces of the column (see Fig. 4). The readings of indicators installed on the end surface to determine the average strains of concrete in the compressed zone (the outermost fiber of the section) should be considered as overestimated by approximately 25% due to the indicator being located 30 mm from the outermost compressed fiber. Therefore, Fig. 7 (number 1) shows the results extrapolated from the experimental strain values of tensile and compressed reinforcement based on the law of plane sections.

For comparison, Fig. 7 shows the calculation results obtained using the stepwise method described above. The experimental strain characteristics and analytical dependencies approximating them, given in [47], were taken as the initial data for the calculation. As can be seen from examining the curves in the figure, there is satisfactory agreement between the results. The calculated values are slightly higher than the experimental ones, which can be partly explained by the fact that the averaged strains are recorded in the experiment, while in the calculations, the strains were obtained in the cross-section with a crack. It is also impossible to exclude some in-fluence of room temperature changes on the creep of concrete. The relatively low increase in strains over time is due to the low level of compressive stresses in concrete and, accordingly, the linear nature of creep.

Fig. 8 shows experimental data on changes in column deflections over time, measured in the middle part of its height. As previously noted for concrete and reinforcement average strains, the measured deflections are total, i.e., include both deflections from an external load with a conditionally instantaneous application and deflections caused by strains of shrinkage and creep of concrete.

In fig. 8, the experimental values of deflections are compared with the calculated ones, obtained using expressions (9) and (10) considering (11). It should be noted that, despite the fact that the calculations do not take into account concrete shrinkage strains, the results are quite satisfactory. Although these strains are small (when the concrete is 90 days old at the time of

loading), they could nevertheless affect the magnitude of the deflections.

The crack opening width in the tensile concrete zone, measured in the middle part of the column height, was 0.05 mm when the column was loaded with a full compressive force (66 kN) and a loading duration of approximately 1 hour. The moment of crack formation corresponded to the moment during the period of loading with a compressive force of up to 40 kN (the previous load level was 30 kN). During the observation period, the crack opening width increased slightly, and after 245 days of being under load, the crack width was approximately 0.06 mm.

Table 4 shows the values of the crack opening width a_{crc} and coefficient ψ_s depending on the duration of the load obtained by calculation. As can be seen, over a period of 245 days, the coefficient ψ_s values changed very little, and the crack opening width increased by approximately 12% and, at the same time, practically stabilized. In addition, calculated values of the crack opening width itself agree quite well with experimental data, considering measurement inaccuracies and the approximate nature of the calculation formulas. Russian Building Codes SP 63.13330.2018 [48] assumes an increase in opening under prolonged load action by 40% compared to short-term action. This difference is not surprising since the standards are focused on a certain margin of crack resistance and cannot consider the specifics of each structure.

Table 4. Values of crack opening width a_{crc} and coefficient ψ_s

Time since loading, (days)	Coefficient ψ_s	a_{crc}, mm	ε_s x 10^5
0	0.8748	0.0451	97.10
1	0.8758	0.0455	97.86
7	0.8783	0.0466	99.96
28	0.8813	0.0479	102.42
70	0.8843	0.0493	105.06
100	0.8857	0.0500	106.36
160	0.8873	0.0508	107.87
245	0.8883	0.0514	108.89

CONCLUSIONS

This study aimed to investigate the behavior of eccentrically loaded reinforced concrete elements made of high strength with mineral additives concrete under prolonged loading and to compare experimental data with theoretical data obtained using a stepwise version of the elastic solutions method. The behavior of eccentrically loaded reinforced concrete elements was studied on a reinforced concrete column. Comparison was made for stresses and strains in the compressed zone of concrete, as well as in tensile and compressed reinforcement. In addition, a comparison was made of the experimental and calculated values of the maximum deflections and crack opening width, which allows us to formulate the following conclusions.

1. The relatively low increase in strains over time is due to the low level of compressive stresses in concrete and, accordingly, the linear nature of creep. A certain excess of the calculated values of strains of the compressed zone of concrete, tensile, and compressed reinforcement over the corresponding experimental values was obtained. This excess is probably explained by the fact that in the experiments, the averaged strains were recorded along the length of the section between the cracks, while in the calculations, strains were obtained for the cross-section with a crack.
2. A comparison of the experimental values of deflections with the values obtained by calculation based on the deformed state in accordance with (9) - (11) showed quite satisfactory agreement with the results.
3. For the first time, using a stepwise version of the method of elastic solutions, the calculation of the opening width of normal cracks for elements made of high-strength concrete with a mineral additive was carried out according to formulas (2), (3), (6) - (11). The calculation results are in good agreement with the experiments and show a significantly smaller increase in crack opening over time compared to that calculated according to Russian Building Codes SP 63.13330.2018.

REFERENCES

1. **Mahmoud, K.A., Abdel Raheem, S.E. and Mansour, M.H.** (2024) Deformational Behavior of Eccentrically Loaded Slender RC Columns Subjected to Sustained Loads. Structures, Elsevier, 59, 105675. https://doi.org/10.1016/J.ISTRUC.2023.105675.
2. **Vasilenko, A., Chernogorsky, D., Strakhov, D. and Sinyakov, L.** (2019) High-Strength Concrete Eccentrically Compressed Elements. E3S Web of Conferences, EDP Sciences, 140. https://doi.org/10.1051/E3SCONF/201914002017.
3. **Harinadha Reddy, D. Ramaswamy, A**. (2018) Experimental and Numerical Modeling of Creep in Different Types of Concrete. Heliyon, Elsevier, 4, e00698. https://doi.org/10.1016/J.HELIYON.2018.E00698.
4. **Liu, Z., Takasu, K., Koyamada, H. and Suyama, H.** (2022) A Study on Engineering Properties and Environmental Impact of Sustainable Concrete with Fly Ash or GGBS. Construction and Building Materials, Elsevier, 316, 125776. https://doi.org/10.1016/J.CONBUILDMAT.2021.125776.
5. **Liu, Y., Li, Y., Mu, J., Li, H. and Shen, J.** (2023) Modeling and Analysis of Creep in Concrete Containing Supplementary Cementitious Materials Based on Machine Learning. Construction and Building Materials, Elsevier, 392, 131911. https://doi.org/10.1016/J.CONBUILDMAT.2023.131911.
6. **Gedam, B.A., Bhandari, N.M. and Upadhyay, A.** (2015) Influence of Supplementary Cementitious Materials on Shrinkage, Creep, and Durability of High-Performance Concrete. Journal of Materials in Civil Engineering, American Society of Civil Engineers, 28, 04015173. https://doi.org/10.1061/(ASCE)MT.1943-5533.0001462.
7. **Li, Y., Liu, Y., Li, Y., Li, Y. and Wang, R.** (2021) Evaluation of Concrete Creep Properties Based on Indentation Test and Multiscale Homogenization Method. Cement and Concrete Composites, Elsevier, 123, 104135. https://doi.org/10.1016/J.CEMCONCOMP.2021.104135.
8. **Korsun, V., Baranov, A., Khon, K. and Ha, Q.** (2021) The Influence of Temperature and Duration of Heating on the Properties of High-Strength Concrete Modified by Organo-Mineral Components. Lecture Notes in Civil Engineering, Springer Science and Business Media Deutschland GmbH, 150 LNCE, 515–524. https://doi.org/10.1007/978-3-030-72404-7_50.
9. **Cao, J., Zeng, P., Liu, T. and Tu, B.** (2023) Influence of Mineral Powder Content and Loading Age on Creep Behavior of Concrete Members under Axial Compression. Results in Engineering, Elsevier, 19, 101304. https://doi.org/10.1016/J.RINENG.2023.101304.
10. **Tangadagi, R.B., M, M., Seth, D. and S, P.** (2021) Role of Mineral Admixtures on Strength and Durability of High Strength Self Compacting Concrete: An Experimental Study. Materialia, Elsevier, 18, 101144. https://doi.org/10.1016/J.MTLA.2021.101144.
11. **He, Z., Qian, C., Li, L. and Du, S.** (2016) Creep Analysis of Concrete with Different Mineral Admixtures. Materials Express, American Scientific Publishers, 6, 328–336. https://doi.org/10.1166/MEX.2016.1319.
12. **Usanova, K., Barabanshchikov, Y.G., Krasova, A. V., Akimov, S. V. and Belyaeva, S. V.** (2021) Plastic Shrinkage of Concrete Modified by Metakaolin. Magazine of Civil Engineering, St. Petersburg Polytechnic University of Peter the Great, 103, 10314–10314. https://doi.org/10.34910/MCE.103.14.
13. **Faridmehr, I., Shariq, M., Plevris, V. and Aalimahmoody, N.** (2022) Novel Hybrid Informational Model for Predicting the Creep and Shrinkage Deflection of Reinforced Concrete Beams Containing GGBFS. Neural Computing and Applications, Springer Science and

Business Media Deutschland GmbH, 34, 13107–13123. https://doi.org/10.1007/S00521-022-07150-3/FIGURES/10.

14. **Shariq, M., Prasad, J. and Abbas, H.** (2016) Creep and Drying Shrinkage of Concrete Containing GGBFS. Cement and Concrete Composites, Elsevier, 68, 35–45. https://doi.org/10.1016/J.CEMCONCOMP.2016.02.004.
15. **Pena, P.V.C., Ferreira, R.A. dos R., Santos, A.C. dos and Oliveira, A.M. de.** (2023) Analysis of the Compressive Creep Strain of the Concretes with Steel Fibers: A Holistic View in Micro and Macro Scale. Journal of Building Engineering, Elsevier, 71, 106436. https://doi.org/10.1016/J.JOBE.2023.106436.
16. **Chen, P., Zheng, W., Wang, Y. and Chang, W.** (2018) Analysis and Modelling of Shrinkage and Creep of Reactive Powder Concrete. Applied Sciences (Switzerland), MDPI AG, 8. https://doi.org/10.3390/APP8050732.
17. **González, L., Gaute, Á., Rico, J. and Thomas, C.** (2021) Effect of Fibre Reinforcement on Creep in Early Age Concrete. Applied Sciences 2022, Vol. 12, Page 257, Multidisciplinary Digital Publishing Institute, 12, 257. https://doi.org/10.3390/APP12010257
18. **Zhao, Q., Yu, J., Geng, G., Jiang, J. and Liu, X.** (2016) Effect of Fiber Types on Creep Behavior of Concrete. Construction and Building Materials, Elsevier, 105, 416–422. https://doi.org/10.1016/J.CONBUILDMAT.2015.12.149.
19. **Kleshchevnikova, V., Belyaeva, S. and Baranov, A.** (2021) Optimization of Mix Designs and Experimental Study of the Properties of Concrete Mix for 3D Printing. Lecture Notes in Civil Engineering, Springer Science and Business Media Deutschland GmbH, 150 LNCE, 151–160. https://doi.org/10.1007/978-3-030-72404-7_16.
20. **Nakararoj, N., Nhat Ho Tran, T., Sukontasukkul, P., Attachaiyawuth, A., Tangchirapat, W., Chee Ban, C., Rattanachu, P. and Jaturapitakkul, C.** (2022) Effects of High-Volume Bottom Ash on Strength, Shrinkage, and Creep of High-Strength Recycled Concrete Aggregate. Construction and Building Materials, Elsevier, 356, 129233. https://doi.org/10.1016/J.CONBUILDMAT.2022.129233.
21. **He, Z.** (2023) Creep and Shrinkage Performance of High-Performance Recycled Aggregate Concrete. Multi-functional Concrete with Recycled Aggregates, Woodhead Publishing, 145–177. https://doi.org/10.1016/B978-0-323-89838-6.00012-8.
22. **Bompa, D. V. and Elghazouli, A.Y.** (2019) Creep Properties of Recycled Tyre Rubber Concrete. Construction and Building Materials, Elsevier, 209, 126–134. https://doi.org/10.1016/J.CONBUILDMAT.2019.03.127.
23. **Usanova, K., Vatin, N. and Barabanshchikov, Y.** (2024) Properties of Cold-Bonded Lightweight Aggregate Based on High Calcium Fly Ash. Lecture Notes in Networks and Systems, Springer, Cham, 733, 187–197. https://doi.org/10.1007/978-3-031-37978-9_18.
24. **Gesoğlu, M., Özturan, T. and Güneyisi, E.** (2006) Effects of Cold-Bonded Fly Ash Aggregate Properties on the Shrinkage Cracking of Lightweight Concretes. Cement and Concrete Composites, Elsevier, 28, 598–605. https://doi.org/10.1016/J.CEMCONCOMP.2006.04.002.
25. **Chen, P., Zhang, G., Cao, S., Lv, X. and Shen, B.** (2023) Creep and Post-Creep Mechanical Properties of Reinforced Concrete Columns. Journal of Building Engineering, Elsevier, 63, 105521. https://doi.org/10.1016/J.JOBE.2022.105521.
26. **Cao, G., Yang, L., Zhang, K. and Peng, X.** (2017) Analysis of Reinforcement

Influence on Concrete Creep. Zhongnan Daxue Xuebao (Ziran Kexue Ban)/Journal of Central South University (Science and Technology), Central South University of Technology, 48, 506–511. https://doi.org/10.11817/J.ISSN.1672-7207.2017.02.031.

27. **Shariff, M.N., Menon, D. and Saravanan, U.** (2023) Experimental and Analytical Studies on Shrinkage and Creep Behavior of RC Walls and Prisms. Structural Concrete, John Wiley and Sons Inc, 24, 6157–6169. https://doi.org/10.1002/SUCO.202300170.
28. **Eom, T.S., Kim, C.S., Zhang, X. and Kim, J.Y.** (2018) Time-Dependent Deformations of Eccentrically Loaded Reinforced Concrete Columns. International Journal of Concrete Structures and Materials, Korea Concrete Institute, 12, 1–12. https://doi.org/10.1186/S40069-018-0312-1/FIGURES/11.
29. **Rhodes, J.A., Carreira, D.J., Bazant, Z.P., Beaudoin, J.I., Branson, D.E., Gamble, B.R., Gcymaycr, H.G., Goyal, B.B., Hope, B.B., Keeton, J.R., Kesler, C.E., Lorman, W.R., Means, J.A., Meyers, B.L., Hills, R.H., Nasser, K.H., Neville, A.H., Roll, F., Timusk, J. and Hard, M.A.** (1982) Prediction of Creep, Shrinkage, and Temperature Effects in Concrete Structures: Reported by ACI Committee 209. American Concrete Institute, ACI Special Publication, American Concrete Institute, 193–300.
30. **Zhou, Y., Chen, W. and Yan, P.** (2022) Measurement and Modeling of Creep Property of High-Strength Concrete Considering Stress Relaxation Effect. Journal of Building Engineering, Elsevier, 56, 104726. https://doi.org/10.1016/J.JOBE.2022.104726.
31. **Wicke, M., Siviero, E., Hilsdorf, H., Müller, H.S., Walraven, J. and Foraboschi, P.** (1999) Structural Concrete. Textbook on Behaviour, Design and Performance. Updated Knowledge of the CEB/FIP Model Code 1990. Volume 1: Introduction-Design Process-Materials. Bulletin-FIB, 1.
32. **Gardner, N.J. and Lockman, M.J.** (2001) Design Provisions for Drying Shrinkage and Creep of Normal-Strength Concrete. Materials, 98, 159–167. https://doi.org/10.14359/10199.
33. **Bažant, Z., Jirasek, M.** (2015) RILEM Draft Recommendation: TC-242-MDC Multi-Decade Creep and Shrinkage of Concrete: Material Model and Structural Analysis. Model B4 for Creep, Drying., CarolMaterials and structures. https://doi.org/10.1617/s11527-014-0485-2.
34. **Huang, Y., Wang, J., Wei, Q., Shang, H. and Liu, X.** (2023) Creep Behaviour of Ultra-High-Performance Concrete (UHPC): A Review. Journal of Building Engineering, Elsevier, 69, 106187. https://doi.org/10.1016/J.JOBE.2023.106187.
35. **Liu, Y., Wang, L., Wei, Y., Sun, C. and Xu, Y.** (2024) Current Research Status of UHPC Creep Properties and the Corresponding Applications – A Review. Construction and Building Materials, Elsevier, 416, 135120. https://doi.org/10.1016/J.CONBUILDMAT.2024.135120.
36. **Hamed, E. and Lai, C.** (2016) Geometrically and Materially Nonlinear Creep Behaviour of Reinforced Concrete Columns. Structures, Elsevier, 5, 1–12. https://doi.org/10.1016/J.ISTRUC.2015.07.001.
37. **Mussabayev, T.T., Nuguzhinov, Z.S., Nemova, D., Kayupov, T., Tolkynbaev, T.A., Akmakanova, A.Z. and Khafizova, G.S.** (2023) Creep of Concrete in Shell Structures: Nonlinear Theory. Materials 2023, Vol. 16, Page 5587, Multidisciplinary Digital Publishing Institute, 16, 5587. https://doi.org/10.3390/MA16165587
38. **Travush, V.I., Kaprielov, S.S., Konin, D. V., Krylov, A.S. and Chilin, I.A.** (2017) Experimental Study of Composite Structures for Bending Elements. Building

and Reconstruction, 63–71. https://doi.org/ZHHHJJ.
39. **Travush, V.I., Karpenko, N.I., Kolchunov, V.I., Kaprielov, S.S., Demyanov, A.I., Bulkin, S.A. and Moskovtseva, V.S.** (2020) Results of Experimental Studies of High-Strength Fiber Reinforced Concrete Beams with Round Cross-Sections under Combined Bending and Torsion. Structural Mechanics of Engineering Constructions and Buildings, Peoples' Friendship University of Russia, 16, 290–297. https://doi.org/10.22363/1815-5235-2020-16-4-290-297.
40. **Travush, V.I., Karpenko, N.I., Kolchunov, V.I., Kaprielov, S.S., Dem'yanov, A.I. and Konorev, A. V.** (2019) Main Results of Experimental Studies of Reinforced Concrete Structures of High-Strength Concrete B100 Round and Circular Cross Sections in Torsion with Bending. Structural Mechanics of Engineering Constructions and Buildings, Peoples' Friendship University of Russia, 15, 51–61. https://doi.org/10.22363/1815-5235-2019-15-1-51-61.
41. **Korsun, V.I., Morozov, V.I., Tamrazyan, A.G. and Alekseytsev, A. V.** (2023) Nonlinear Deformation Model for Analysis of Temperature Effects on Reinforced Concrete Beam Elements. Buildings 2023, Vol. 13, Page 2734, Multidisciplinary Digital Publishing Institute, 13, 2734. https://doi.org/10.3390/BUILDINGS13112734.
42. **Vorobeva, A., Strakhov, D. and Semenov, K.** (2021) Calculation of Reinforced Concrete Elements Taking into Account Nonlinear Creep at Different Loading Mode. Lecture Notes in Civil Engineering, Springer Science and Business Media Deutschland GmbH, 150 LNCE, 73–84. https://doi.org/10.1007/978-3-030-72404-7_8/TABLES/5.
43. **Bezgodov, I., Kaprielov, S. and Sheynfeld, A.** (2023) Relationship Between Strength and Deformation Characteristics of High-Strength Self-Compacting Concrete. Lecture Notes in Civil Engineering, Springer Science and Business Media Deutschland GmbH, 282, 459–468. https://doi.org/10.1007/978-3-031-10853-2_43/FIGURES/4.
44. International Technical Standard GOST 10181-2014. Concrete Mixtures. Methods of Testing. Russian Federation. https://docs.cntd.ru/document/1200115733?section=text.
45. International Technical Standard GOST 10180-2012. Concretes. Methods for Strength Determination Using Reference Specimens. Russian Federation. https://docs.cntd.ru/document/1200100908.
46. International Technical Standard GOST 24452-80 Concretes. Methods of Prismatic, Compressive Strength, Modulus of Elasticity and Poisson's Ratio Determination. Russian Federation. https://kodeks.library.spbstu.ru/docs/
47. **Baranov, A.O. and Strakhov, D.A.** (2023) Creep of High Strength Concrete at Elevated Temperatures. Construction of Unique Buildings and Structures, 108, 10704–10704. https://doi.org/10.4123/CUBS.107.4.
48. Russian Building Codes SP 63.13330.2018. Concrete and Reinforced Concrete Structures. General Provisions. Russian Federation. https://docs.cntd.ru/document/554403082.

СПИСОК ЛИТЕРАТУРЫ

1. **Mahmoud, K.A., Abdel Raheem, S.E. and Mansour, M.H.** (2024) Deformational Behavior of Eccentrically Loaded Slender RC Columns Subjected to Sustained Loads. Structures, Elsevier, 59, 105675. https://doi.org/10.1016/J.ISTRUC.2023.105675.
2. **Vasilenko, A., Chernogorsky, D., Strakhov, D. and Sinyakov, L.** (2019) High-Strength Concrete Eccentrically Compressed Elements. E3S Web of

Conferences, EDP Sciences, 140. https://doi.org/10.1051/E3SCONF/201914002017.

3. **Harinadha Reddy, D. Ramaswamy, A**. (2018) Experimental and Numerical Modeling of Creep in Different Types of Concrete. Heliyon, Elsevier, 4, e00698. https://doi.org/10.1016/J.HELIYON.2018.E00698.
4. **Liu, Z., Takasu, K., Koyamada, H. and Suyama, H.** (2022) A Study on Engineering Properties and Environmental Impact of Sustainable Concrete with Fly Ash or GGBS. Construction and Building Materials, Elsevier, 316, 125776. https://doi.org/10.1016/J.CONBUILDMAT.2021.125776.
5. **Liu, Y., Li, Y., Mu, J., Li, H. and Shen, J.** (2023) Modeling and Analysis of Creep in Concrete Containing Supplementary Cementitious Materials Based on Machine Learning. Construction and Building Materials, Elsevier, 392, 131911. https://doi.org/10.1016/J.CONBUILDMAT.2023.131911.
6. **Gedam, B.A., Bhandari, N.M. and Upadhyay, A.** (2015) Influence of Supplementary Cementitious Materials on Shrinkage, Creep, and Durability of High-Performance Concrete. Journal of Materials in Civil Engineering, American Society of Civil Engineers, 28, 04015173. https://doi.org/10.1061/(ASCE)MT.1943-5533.0001462.
7. **Li, Y., Liu, Y., Li, Y., Li, Y. and Wang, R.** (2021) Evaluation of Concrete Creep Properties Based on Indentation Test and Multiscale Homogenization Method. Cement and Concrete Composites, Elsevier, 123, 104135. https://doi.org/10.1016/J.CEMCONCOMP.2021.104135.
8. **Korsun, V., Baranov, A., Khon, K. and Ha, Q.** (2021) The Influence of Temperature and Duration of Heating on the Properties of High-Strength Concrete Modified by Organo-Mineral Components. Lecture Notes in Civil Engineering, Springer Science and Business Media Deutschland GmbH, 150 LNCE, 515–524. https://doi.org/10.1007/978-3-030-72404-7_50.
9. **Cao, J., Zeng, P., Liu, T. and Tu, B.** (2023) Influence of Mineral Powder Content and Loading Age on Creep Behavior of Concrete Members under Axial Compression. Results in Engineering, Elsevier, 19, 101304. https://doi.org/10.1016/J.RINENG.2023.101304.
10. **Tangadagi, R.B., M, M., Seth, D. and S, P.** (2021) Role of Mineral Admixtures on Strength and Durability of High Strength Self Compacting Concrete: An Experimental Study. Materialia, Elsevier, 18, 101144. https://doi.org/10.1016/J.MTLA.2021.101144.
11. **He, Z., Qian, C., Li, L. and Du, S.** (2016) Creep Analysis of Concrete with Different Mineral Admixtures. Materials Express, American Scientific Publishers, 6, 328–336. https://doi.org/10.1166/MEX.2016.1319.
12. **Usanova, K., Barabanshchikov, Y.G., Krasova, A. V., Akimov, S. V. and Belyaeva, S. V.** (2021) Plastic Shrinkage of Concrete Modified by Metakaolin. Magazine of Civil Engineering, St. Petersburg Polytechnic University of Peter the Great, 103, 10314–10314. https://doi.org/10.34910/MCE.103.14.
13. **Faridmehr, I., Shariq, M., Plevris, V. and Aalimahmoody, N.** (2022) Novel Hybrid Informational Model for Predicting the Creep and Shrinkage Deflection of Reinforced Concrete Beams Containing GGBFS. Neural Computing and Applications, Springer Science and Business Media Deutschland GmbH, 34, 13107–13123. https://doi.org/10.1007/S00521-022-07150-3/FIGURES/10.
14. **Shariq, M., Prasad, J. and Abbas, H.** (2016) Creep and Drying Shrinkage of Concrete Containing GGBFS. Cement and Concrete Composites, Elsevier, 68, 35–45. https://doi.org/10.1016/J.CEMCONCOMP.2016.02.004.

15. **Pena, P.V.C., Ferreira, R.A. dos R., Santos, A.C. dos and Oliveira, A.M. de.** (2023) Analysis of the Compressive Creep Strain of the Concretes with Steel Fibers: A Holistic View in Micro and Macro Scale. Journal of Building Engineering, Elsevier, 71, 106436. https://doi.org/10.1016/J.JOBE.2023.106436.
16. **Chen, P., Zheng, W., Wang, Y. and Chang, W.** (2018) Analysis and Modelling of Shrinkage and Creep of Reactive Powder Concrete. Applied Sciences (Switzerland), MDPI AG, 8. https://doi.org/10.3390/APP8050732.
17. **González, L., Gaute, Á., Rico, J. and Thomas, C.** (2021) Effect of Fibre Reinforcement on Creep in Early Age Concrete. Applied Sciences 2022, Vol. 12, Page 257, Multidisciplinary Digital Publishing Institute, 12, 257. https://doi.org/10.3390/APP12010257
18. **Zhao, Q., Yu, J., Geng, G., Jiang, J. and Liu, X.** (2016) Effect of Fiber Types on Creep Behavior of Concrete. Construction and Building Materials, Elsevier, 105, 416–422. https://doi.org/10.1016/J.CONBUILDMAT.2015.12.149.
19. **Kleshchevnikova, V., Belyaeva, S. and Baranov, A.** (2021) Optimization of Mix Designs and Experimental Study of the Properties of Concrete Mix for 3D Printing. Lecture Notes in Civil Engineering, Springer Science and Business Media Deutschland GmbH, 150 LNCE, 151–160. https://doi.org/10.1007/978-3-030-72404-7_16.
20. **Nakararoj, N., Nhat Ho Tran, T., Sukontasukkul, P., Attachaiyawuth, A., Tangchirapat, W., Chee Ban, C., Rattanachu, P. and Jaturapitakkul, C.** (2022) Effects of High-Volume Bottom Ash on Strength, Shrinkage, and Creep of High-Strength Recycled Concrete Aggregate. Construction and Building Materials, Elsevier, 356, 129233. https://doi.org/10.1016/J.CONBUILDMAT.2022.129233.
21. **He, Z.** (2023) Creep and Shrinkage Performance of High-Performance Recycled Aggregate Concrete. Multi-functional Concrete with Recycled Aggregates, Woodhead Publishing, 145–177. https://doi.org/10.1016/B978-0-323-89838-6.00012-8.
22. **Bompa, D. V. and Elghazouli, A.Y.** (2019) Creep Properties of Recycled Tyre Rubber Concrete. Construction and Building Materials, Elsevier, 209, 126–134. https://doi.org/10.1016/J.CONBUILDMAT.2019.03.127.
23. **Usanova, K., Vatin, N. and Barabanshchikov, Y.** (2024) Properties of Cold-Bonded Lightweight Aggregate Based on High Calcium Fly Ash. Lecture Notes in Networks and Systems, Springer, Cham, 733, 187–197. https://doi.org/10.1007/978-3-031-37978-9_18.
24. **Gesoğlu, M., Özturan, T. and Güneyisi, E.** (2006) Effects of Cold-Bonded Fly Ash Aggregate Properties on the Shrinkage Cracking of Lightweight Concretes. Cement and Concrete Composites, Elsevier, 28, 598–605. https://doi.org/10.1016/J.CEMCONCOMP.2006.04.002.
25. **Chen, P., Zhang, G., Cao, S., Lv, X. and Shen, B.** (2023) Creep and Post-Creep Mechanical Properties of Reinforced Concrete Columns. Journal of Building Engineering, Elsevier, 63, 105521. https://doi.org/10.1016/J.JOBE.2022.105521.
26. **Cao, G., Yang, L., Zhang, K. and Peng, X.** (2017) Analysis of Reinforcement Influence on Concrete Creep. Zhongnan Daxue Xuebao (Ziran Kexue Ban)/Journal of Central South University (Science and Technology), Central South University of Technology, 48, 506–511. https://doi.org/10.11817/J.ISSN.1672-7207.2017.02.031.
27. **Shariff, M.N., Menon, D. and Saravanan, U.** (2023) Experimental and Analytical

Studies on Shrinkage and Creep Behavior of RC Walls and Prisms. Structural Concrete, John Wiley and Sons Inc, 24, 6157–6169. https://doi.org/10.1002/SUCO.202300170.

28. **Eom, T.S., Kim, C.S., Zhang, X. and Kim, J.Y.** (2018) Time-Dependent Deformations of Eccentrically Loaded Reinforced Concrete Columns. International Journal of Concrete Structures and Materials, Korea Concrete Institute, 12, 1–12. https://doi.org/10.1186/S40069-018-0312-1/FIGURES/11.
29. **Rhodes, J.A., Carreira, D.J., Bazant, Z.P., Beaudoin, J.I., Branson, D.E., Gamble, B.R., Gcymaycr, H.G., Goyal, B.B., Hope, B.B., Keeton, J.R., Kesler, C.E., Lorman, W.R., Means, J.A., Meyers, B.L., Hills, R.H., Nasser, K.H., Neville, A.H., Roll, F., Timusk, J. and Hard, M.A.** (1982) Prediction of Creep, Shrinkage, and Temperature Effects in Concrete Structures: Reported by ACI Committee 209. American Concrete Institute, ACI Special Publication, American Concrete Institute, 193–300.
30. **Zhou, Y., Chen, W. and Yan, P.** (2022) Measurement and Modeling of Creep Property of High-Strength Concrete Considering Stress Relaxation Effect. Journal of Building Engineering, Elsevier, 56, 104726. https://doi.org/10.1016/J.JOBE.2022.104726.
31. **Wicke, M., Siviero, E., Hilsdorf, H., Müller, H.S., Walraven, J. and Foraboschi, P.** (1999) Structural Concrete. Textbook on Behaviour, Design and Performance. Updated Knowledge of the CEB/FIP Model Code 1990. Volume 1: Introduction-Design Process-Materials. Bulletin-FIB, 1.
32. **Gardner, N.J. and Lockman, M.J.** (2001) Design Provisions for Drying Shrinkage and Creep of Normal-Strength Concrete. Materials, 98, 159–167. https://doi.org/10.14359/10199.
33. **Bažant, Z., Jirasek, M.** (2015) RILEM Draft Recommendation: TC-242-MDC Multi-Decade Creep and Shrinkage of Concrete: Material Model and Structural Analysis. Model B4 for Creep, Drying., CarolMaterials and structures. https://doi.org/10.1617/s11527-014-0485-2.
34. **Huang, Y., Wang, J., Wei, Q., Shang, H. and Liu, X.** (2023) Creep Behaviour of Ultra-High-Performance Concrete (UHPC): A Review. Journal of Building Engineering, Elsevier, 69, 106187. https://doi.org/10.1016/J.JOBE.2023.106187.
35. **Liu, Y., Wang, L., Wei, Y., Sun, C. and Xu, Y.** (2024) Current Research Status of UHPC Creep Properties and the Corresponding Applications – A Review. Construction and Building Materials, Elsevier, 416, 135120. https://doi.org/10.1016/J.CONBUILDMAT.2024.135120.
36. **Hamed, E. and Lai, C.** (2016) Geometrically and Materially Nonlinear Creep Behaviour of Reinforced Concrete Columns. Structures, Elsevier, 5, 1–12. https://doi.org/10.1016/J.ISTRUC.2015.07.001.
37. **Mussabayev, T.T., Nuguzhinov, Z.S., Nemova, D., Kayupov, T., Tolkynbaev, T.A., Akmakanova, A.Z. and Khafizova, G.S.** (2023) Creep of Concrete in Shell Structures: Nonlinear Theory. Materials 2023, Vol. 16, Page 5587, Multidisciplinary Digital Publishing Institute, 16, 5587. https://doi.org/10.3390/MA16165587
38. **Травуш В.И., Каприелов С.С., Конин Д.В., Крылов А.С., Чилин И.А.** Экспериментальные исследования сталежелезобетонных конструкций, работающих на изгиб // Строительство и реконструкция, 2017, №4 (72). С.63-71.
39. **Травуш В.И., Карпенко Н.И., Колчунов В.И., и др.** Результаты экспериментальных исследований сложнонапряженных балок круглого поперечного сечения из высокопрочного фиброжелезобетона // Строительная

механика инженерных конструкций и сооружений, 2020. Т. 16. №4. С. 290-297. doi: 10.22363/1815-5235-2020-16-4-290-297

40. **Травуш В.И., Карпенко Н.И., Колчунов В.И., и др.** Основные результаты экспериментальных исследований железобетонных конструкций из высокопрочного бетона В100 круглого и кольцевого сечений при кручении с изгибом // Строительная механика инженерных конструкций и сооружений, 2019, Т. 15. №1. С. 51-61 https://doi.org/10.22363/1815-5235-2019-15-1-51-61.
41. **Korsun, V.I., Morozov, V.I., Tamrazyan, A.G. and Alekseytsev, A. V.** (2023) Nonlinear Deformation Model for Analysis of Temperature Effects on Reinforced Concrete Beam Elements. Buildings 2023, Vol. 13, Page 2734, Multidisciplinary Digital Publishing Institute, 13, 2734. https://doi.org/10.3390/BUILDINGS13112734.
42. **Vorobeva, A., Strakhov, D. and Semenov, K.** (2021) Calculation of Reinforced Concrete Elements Taking into Account Nonlinear Creep at Different Loading Mode. Lecture Notes in Civil Engineering, Springer Science and Business Media Deutschland GmbH, 150 LNCE, 73–84. https://doi.org/10.1007/978-3-030-72404-7_8/TABLES/5.
43. **Bezgodov, I., Kaprielov, S. and Sheynfeld, A.** (2023) Relationship Between Strength and Deformation Characteristics of High-Strength Self-Compacting Concrete. Lecture Notes in Civil Engineering, Springer Science and Business Media Deutschland GmbH, 282, 459–468. https://doi.org/10.1007/978-3-031-10853-2_43/FIGURES/4.
44. ГОСТ 10181-2014. Смеси бетонные. Методы испытаний. https://docs.cntd.ru/document/1200115733?section=text.
45. ГОСТ 10180-2012. Бетоны. Методы определения прочности по контрольным образцам. https://docs.cntd.ru/document/1200100908.
46. ГОСТ 24452-80. Бетоны. Методы определения призменной прочности, модуля упругости и коэффициента Пуассона. https://kodeks.library.spbstu.ru/docs/
47. **Baranov, A.O. and Strakhov, D.A.** (2023) Creep of High Strength Concrete at Elevated Temperatures. Construction of Unique Buildings and Structures, 108, 10704–10704. https://doi.org/10.4123/CUBS.107.4.
48. СП 63.13330.2018. Бетонные и железобетонные конструкции. Основные положения. https://docs.cntd.ru/document/554403082.

Dmitry Alexandrovich Strakhov, Candidate of Technical Sciences, Assistant Professor at Higher School of Industrial, Civil and Road Construction, Peter the Great St. Petersburg Polytechnic University, Russia, St. Petersburg, 195251, Politechnicheskaya str., 29B, sdaleks2008@rambler.ru

Aleksey Olegovich Baranov, Senior Lecturer at the Higher School of Industrial, Civil and Road Construction, Peter the Great St. Petersburg Polytechnic University, Russia, St. Petersburg, 195251, Politechnicheskaya str., 29B, baranov_ao@spbstu.ru

Дмитрий Александрович Страхов, кандидат технических наук, доцент, доцент Высшей школы промышленно-гражданского и дорожного строительства (ВШПГиДС), Санкт-Петербургский политехнический университет Петра Великого (СПбПУ), Россия, Санкт-Петербург, 195251, ул. Политехническая, д. 29 литера Б, sdaleks2008@rambler.ru

Алексей Олегович Баранов, старший преподаватель Высшей школы промышленно-гражданского и дорожного строительства (ВШПГиДС), Санкт-Петербургский политехнический университет Петра Великого (СПбПУ), Россия, Санкт-Петербург, 195251, ул. Политехническая, д. 29 литера Б, baranov_ao@spbstu.ru

International Journal for Computational Civil and Structural Engineering, 20(4) 160–171(2024)

DOI:10.22337/2587-9618-2024-20-4-160-171

NUMERICAL INVESTIGATION ON FLEXURAL PERFORMANCE OF BUILT-UP STEEL BEAMS WITH DIFFERENT WEB OPENINGS

Hussein Talab Nhabih [1], Mohammad R.K.M. Al-Badkubi [2], Marwa Marza Salman [3]

[1] Department of building and construction technology, Islamic University, Najaf, IRAQ
[2] Department of Civil Engineering, Faculty of Engineering, Babylon University, Babylon, IRAQ
[3] Department of Ceramic and Building Material, Faculty of Materials Engineering, Babylon University, Babylon, IRAQ

Abstract. Recently, the usage of Structural Steel Beams with Opening in the Web has spread extensively in all over the world, in various types of buildings such as high-rise buildings and industrial buildings. There are several advantages in using openings in beams. There for, an analytical investigation was carried out on fourSteel Beams with Opening (SBWO) models by using a powerful nonlinear simulation software ABAQUS. The initiative was to study the overall flexural behaviour of (SBWO's) and to establish the maximum load carrying capacity, and deflection. Only vertical loads have been considered in the (SBWO's) performance investigation. The Built-Up sections were tested up to failure. The simulated models were considered to be under simply supported condition at their edges and a uniform distributed load were applied over the upper flange of the beam along all beam's length. The flexural behaviour of beams with different opening shapes were tested and compared. The test results proved to be very useful in selecting the opening shape.

Keywords*:* Finite Element Modeling, Abaqus Computer Program, Flexural Behavior, Built-Up Section, Steel Beam, Web Opening

ЧИСЛЕННОЕ ИССЛЕДОВАНИЕ ИЗГИБА СОСТАВНЫХ СТАЛЬНЫХ БАЛОК С ОТВЕРСТИЯМИ РАЗЛИЧНОЙ ФОРМЫ В СТЕНКЕ

Хусейн Талаб Набих [1], Мохаммад Р.К.М. Аль-Бадкуби [2], Марва Марза Салман [3]

[1] Кафедра строительства и строительных технологий, Исламский университет, Наджаф, ИРАК
[2] Кафедра гражданского строительства, инженерный факультет, Вавилонский университет, Вавилон, ИРАК
[3] Кафедра керамики и строительных материалов, факультет материаловедения, Вавилонский университет, Вавилон, ИРАК

Аннотация. В последнее время использование стальных балок с отверстиями в стенке получило широкое распространение во всем мире, в различных типах зданий, таких как высотные и промышленные здания. Использование отверстий в стенках балок имеет ряд преимуществ. Поэтому было проведено численное исследование четырех моделей стальных балок с отверстиями (SBWO) с помощью программного обеспечения для нелинейного моделирования ABAQUS. Целью исследования было изучение общего сопротивления изгибу балок (SBWO) и определение максимальной несущей способности, а также прогиба. При исследовании характеристик (SBWO) учитывались только вертикальные нагрузки. Нагружение выполнялось вплоть до разрушения. Рассматривались свободно опертые по краям балки. К верхней полке балки по всей ее длине прикладывалась равномерно распределенная нагрузка. Были исследования и сравнение результатов для балок с различными формами отверстий. Полученные результаты исследований могут быть использованы при выборе формы отверстий в стальных двутавровых балках.

Ключевые слова: Конечно-элементное моделирование, компьютерная программа Abaqus, изгиб, составное сечение, стальная балка, отверстие в стенке

I. INTRODUCTION

From about eight decades, a large number of investigations have made by structural engineers looking for an untraditional methods to decrease the charge of steel constructions as much as possible. From designing point of view the maximum potential structural steel strength properties cannot always be achievable due to existence of other design factor such as serviceability. This factor usually accounts in the design process by taking the maximum permissible deflection to be the design factor. Therefore, numerous innovative ways have been suggested to increase the steel member's stiffness without increasing the required weight of steel, significantly.

Thus, steel beams with web opening also known as castellated or cellular beams have been used widely. One of the major benefits of using the openings in the beam in construction is the incorporation of services, such as electric cables as well as ventilation and hydraulic pipes, through the designed section depth of the beams, as shown in Fig.1.

The strength of structural members with web opening has been stated that may have large reduction. This statements were made by researchers like Bower (1968) [2], Lawson (1987) [3], and Darwin (1990) [4].

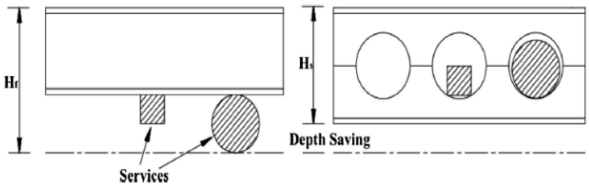

Figure 1. Reduction of beam height by utilizing holes for insertion service combinations [1]

However, the present specifications and design procedure codes for such beams are also difficult to use or inadequate (SCI P355 2011) [5]. This can be because the complexity in understanding and analyzing the performance of steel beams with web openings, and too difficulties to simplify design procedures. Thus, more extensive researches and investigations are needed in order to achieve sufficient information for understanding the behavior of beams with web opening to develop a much simpler design method. There are some analytical and experimental investigations have been made in the past to study SBWOs behavior. Redwood (1969) [6] suggested that by using modified dimensions equivalent rectangular opening, most of the design rules can be applied for steel beams with circular web openings. However, the ultimate strength of steel beams are substantially underestimated as a result of the simplistic approach. Chan and Redwood (1974) [7] used the curved beam analysis and the theory of elasticity to examine stress distribution in elastic range for beams having big circular shape web openings. The investigations made by Olander (1953) [8] and Sahmel (1969) [9] were used to develop a design method at the Steel Building Institute in 1990 in order to find the ultimate strength of steel beams having several circular shape web openings using an explicit approach. Later on in 1998, the method incorporated in Euro code 3 (EN1993-1-3)[10] after minor modification. However, this method also has been recommended to use for steel beams with separate circular shape web openings using a dissimilar set of approximate design methods. Laboratory tests and Numerical investigation on steel beams with circular and rectangular openings have been approved by Thevendran and Shanmugan (1991) [11]. They constructed cantilever and simply supported beams models made from a plexi glass sheet. For computing the critical buckling load for this type of beams the energy technique was proposed. Lawson and Chung (2001) [12] made an theoretical investigation on steel beams having circular and rectangular openings using a large web opening composite beams design method and presented in Euro code 4. Two suggestions were made by Chung et al. (2001) [13] first a practical design method against Vierendeel mechanism for circular web opening steel beams, second the perforated section empirical shear–moment interaction curve. An empirical design method was industrialized by Chung et al. (2003) [14]using generalized moment–shear interaction curve for steel beam

with various shapes and sizes web openings. Tsavdaridic and D'Mello (2011) [15] made a study on the web post buckling effective 'strut' action and guess the final vertical shear load strength of web posts using an empirical formula obtained from the particular shapes of web opening. In order to achieve a simplified approach to develop a reliable prediction for moment modification factor K_{LB} in cellular beams an investigation was made by Sweedan (2011) [16]. An experimental investigation was made by Saka and Erdal (2013) [17] and they observed different types of failure modes including post buckling of the web, Vierendeel bending, web buckling and lateral torsional buckling. A through finite element method was performed by Panedpojaman and Thepchatri (2013) [18] and a modified coefficient function were suggested after analyzing 408 nonlinear finite element model fore liable deflection prediction of cellular beams. A numerical and experimental study was made by Boissonnade et al. (2014) [19] and a design procedure for lateral torsional buckling in cellular beam was suggested. Samadhan and Laxmikant (2015) [1] performed an experimental and parametric study on simply supported steel beams with web opening subjected to vertical loading. Iman Satyarno et al. (2017) [20], perform an analysis on castellated steel beam by full scaled rectangular opening shape in which some of the specimens were partially encased in reinforced mortar and some of them without encasing. Made Sukrawa (2017) [21], made a finite element study on reinforced steel beam with large opening in the web subjected to axial forces. Tareq Almusallam et al. (2018), perform an experimental and numerical investigation on behavior of FRP-strengthened RC beams having large rectangular shape web openings in flexural zones. Morkhade et al. (2019) [23], made an effort on study the effect of opening in the web on the ultimate strength of steel beam by trapezoidal corrugated shape web in which it can increase the share capacity without providing the transverse stiffeners.

There are numerous benefits of using SBWOs, some of them can be listed as:

- Incorporation of services within the structural height of the beams.
- Reduction of overall dead weight of the structure which allows smaller foundation sizes.
- Reducing overall costs due to reduction of material consumption.
- Longer spans between columns than traditional structures.

II. SAMPLES DESCRIPTION

This study signifies an analytical study on flexural performance of built-up section steel beams with different web opening which consists tests on four steel beam models up to failure using a nonlinear simulation software Abaqus to find the better opening type which gives better performance during the application of loading.

In general the test results give an overall understanding of the behavior of these beams. The failure type which controls the behavior of these beams is flexural failure in the section. In the present investigation the load–deflection behavior, the ultimate load-carrying capacity and the failure modes are to be considered. Fig. 2 & 3 illustrated the specification details of the test specimens. These details also listed in Table 1.

As it is shown in Fig.2a-d, for all steel beam specimens the parameters such as beam overall dimensions and total number of the openings and beam's depth were kept constant in order to investigate only the influence of opening shape on the flexural behavior of the steel beams with web opening exclusively. From practical point of view manufacturing circular web opening is the easiest comparing to other shapes because of the drilling, measuring and residual stresses. Thus, the steel beam having circular shape web opening is used to select other opening shapes dimensions and spacing. As shown in the Fig. 2a, 3the diameter of the circular opening is selected so that the opening be large enough to see the effect of the opening on flexural behavior more clearly, and the spacing between the circular openings is calculated according to the design of openings from BS 5950 part-I (2000) [24] which considers to take opening

spacing to its diameter ratio (S/D_o = 1.08–1.5). Also, the web openings considered to start from 250 mm from the ends of the beam. This distance is selected in order to increase the stiffness of the beam at support zone and also not too far from the support so that the opening is spread in all beam's length and practically be possible to use any length for the beam and do not need special manufacturing for different beam's length. Furthermore, to investigate the influence of the opening shape exclusively the dimensions of the other web opening shapes are selected so that the area of the shape remain almost equal to the area of the circular shape. For dissimilar opening shapes for example rectangular, triangular, and hexagonal shape, in order to minimize the high stress concentration which occurs in the opening shape corners, a 5 mm in radius fillet is provided in those regions. As shown in Fig. 2c the spacing between the openings is not large enough to place the triangles with same orientation, so to maintain the opening numbers and spacing the nearby triangle for each opening is flipped upside down.

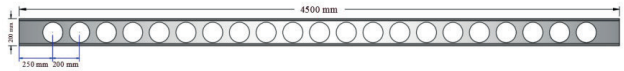

a) Steel beam with circular web opening (SBCWO).

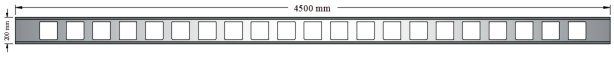

b) Steel beam with square web opening (SBSWO).

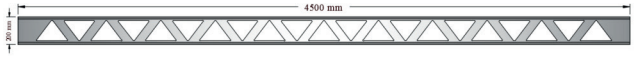

c) Steel beam with triangular web opening (SBTWO).

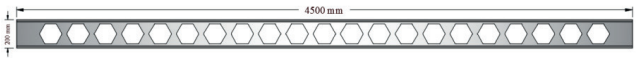

d) Steel beam with hexagonal web opening (SBHWO).

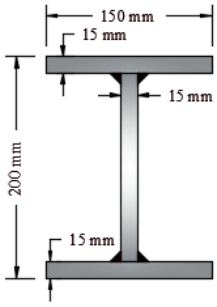

Figure 2. Schematic representation of tested specimens

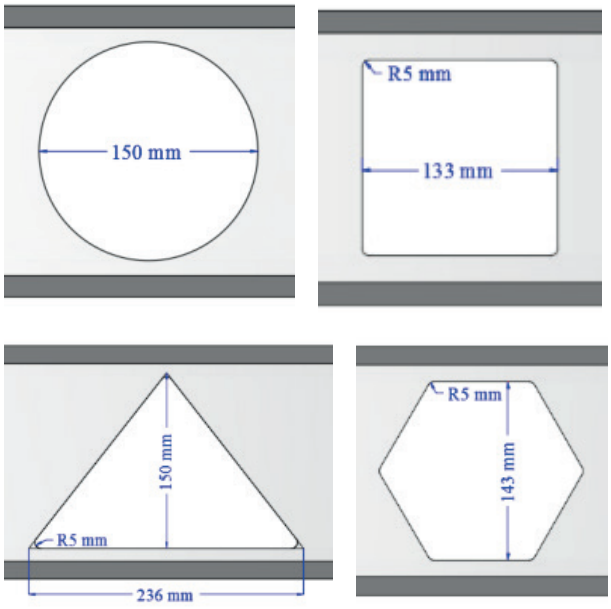

Figure 3. Opening details

Table 1. Samples Identification

No.	Beam Symbol	Length (mm)	Opening Shape	Flange Width (mm)
1	SBCWO	4500	Circular	150
2	SBSWO	4500	Square	150
3	SBTWO	4500	Triangular	150
4	SBHWO	4500	Hexagonal	150

III. FINITE ELEMENT MODELLING OF THE SPECIMENS

The simulated SBWO models have been used to guess ultimate strength capacity and flexural behavior of the samples during the loading time and at the final stage of loading which considered to be the model rupture failure using finite element simulation technique. Thus, a 3-D model with limited finite elements is developed by using a powerful simulation software Abaqus (6.14-4), which can simulate the material properties as well as geometric nonlinearity in beam samples.

Building the models is the starting step in the finite element analysis method. In this step, the

overall structure of the model is formed after that the model divided in to finite elements, each element connected with others at their nodes. It is necessary to define the element type, material properties and overall geometry of the model to build an accurate finite element model. Furthermore, the accuracy and cogency of the adapted sample is verified by comparing the test results to those given by an experimental study made by Samadhan (2015) [1].

A. Modelling of Built-Up Steel Beam with Web Opening

1) Steel Beam Sketch

In order to establish valid and reliable simulated models of the steel beam with web opening the steel beam parts are drew and their characteristics are carefully designated. First, the structure of steel beam is formed after selecting the 3D space modeling, solid extrusion shape, and deformable type, as shown in Fig.4.The beam's cross section dimensions and its length have been simulated according to the specimen identification table shown previously. The simulation of the openings for other types of openings are also done by selecting the 3D space modeling, solid extrusion shape, and deformable type, as shown in Fig.5.

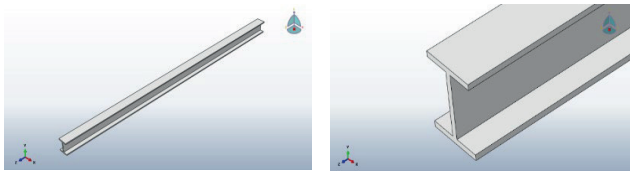

Figure 4. Modelling of solid steel beam part

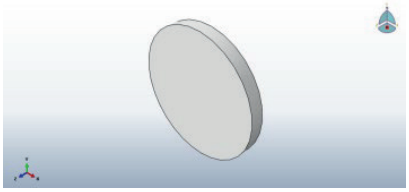

Figure 5. Modelling of solid opening shape part

Finally to achieve the steel beam with web opening models, the solid opening shape part is subtracted from the solid steel beam part. Then, a new complete steel beam with web opening part is created as shown in Fig.6.

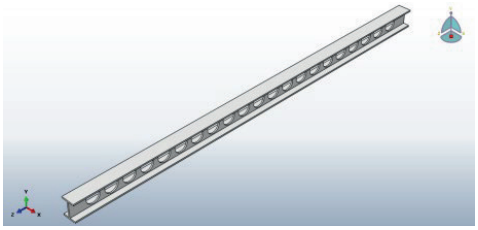

Figure 6. Complete steel beam with web opening model

2) Element Type Selection

In the presented study the element type which adopted to represent the steel beams was a 10-noded 3D stress quadratic tetrahedron elements (C3D10M) which has six degree of freedom at each node. Fig. 7 show the adapted element for steel beams.

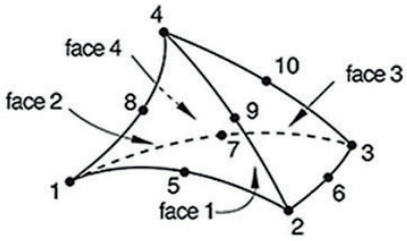

Figure 7. 10-node quadratic tetrahedron element (C3D10M) [25]

The selection of the model mesh density was done in such a way so that each element has the same length of 25mm length. Thus, the total number of element in the beam width are 6 elements and in the length 180 element. Fig. 8 demonstrations the meshed shape of the steel beam.

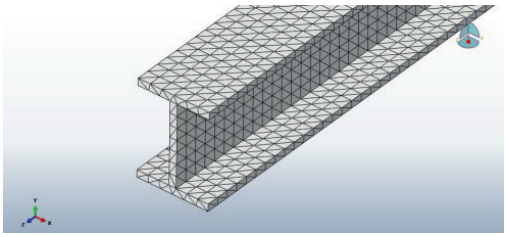

Figure 8. Meshed shape of steel beam model

3) Material Mechanical Properties

The steel material properties in this study taken similar to steel properties in experimental study made by Samadhan (2015) [1], which obtained from tensile test made on a coupons cut of a steel plate. The experiment results such as modulus of elasticity, ultimate stress, and yield stress, are given in Table 2.

Table 2. Properties of Steel Material

f_y (MPa)	f_u (MPa)	E_s (MPa)	υ
350	490	200,000	0.3

A simplified stress–strain curve shown in Fig. 9 is adapted for modelling the steel material mechanical properties along by the von Misses yield criterion having the isotropic hardening law. The adapted properties simulation shown to be adequate in simulating steel material properties due to test results. Also, in here the effect of large deformation have been considered.

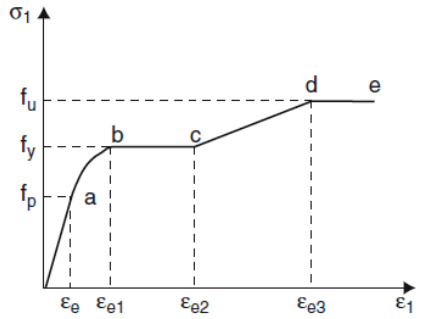

Figure 9. Stress-strain curve for steel [26]

4) Models Boundary Conditions

To make sure of obtaining a unique results in analyzing the deformation and maximum load capacity in the simulated steel beams with web opening the selection of the models end boundary conditions are necessary. In the present research work the steel beams are considered to be simply supported beams. In order to achieve this condition in the simulated models two additional solid extrudes are used at the bottom face of the steel beams. The solid extrudes considered to have rectangular shape with dimensions of (100, 150, 50 mm) in width, length and thickness, respectively. The extrudes considered to be made from hard steel with (f_y = 600 MPa and f_u = 900 MPa), this type of steel is used to ensure that the extrudes will not deform under the ultimate load for the steel beams. The solid extrudes are placed at a distance of 150 mm from the two edges of the steel beams. The left support considered to be hinged support and the right one considered to be roller support. The type of support can be determined by selecting the restricted transition direction. To ensure the nodal action of the supports the center line on the bottom face of the solid extrude are selected to be the line of supports. Fig.10 shows the solid extrude simulation and modelling of the support line location.

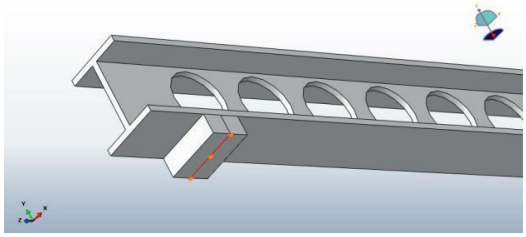

Figure 10. Solid extrude simulation and modelling of the support line location

5) Loading Mechanism

To simulate the applied load on the beam specimen the mechanical pressure type was selected to act on top face of the steel beams as shown in Fig. 11.

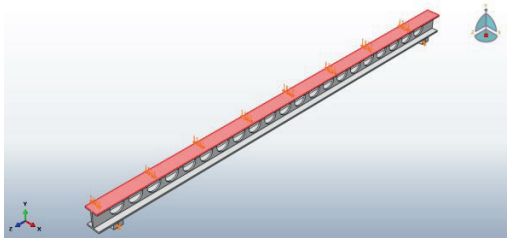

Figure 11. Modelling of loading pressure on top face of the steel beam sample

The applied pressure is distributed evenly at all surface area and increases linearly up to failure of the specimen.

IV. PARAMETRIC STUDY

A parametric study was made after making sure of the accuracy of the used finite element modeling predicting the ultimate load capacity, to investigate the shape of the opening influence on the flexural behavior of steel beams with web openings.

For simulating the other steel beams models with other types opening shapes, similar procedure which was used to simulate the steel beam with circular shape opening in the web model is used. But, with slight difference due to different shapes of the openings. Fig.12 illustrates the other steel beams modeled in Abaqus.

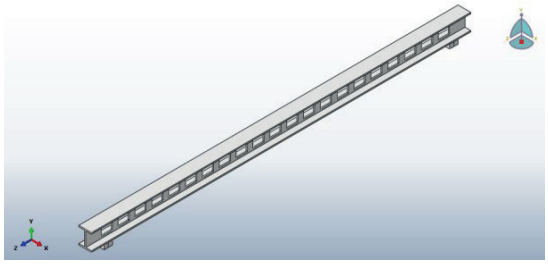

a) Steel Beam with Square Web Opening (SBSWO)

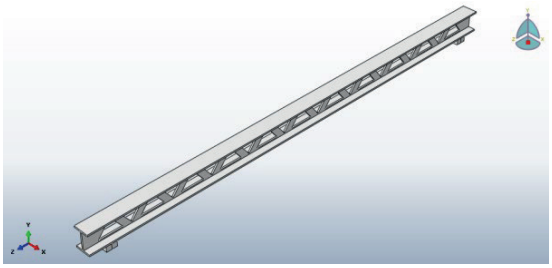

b) Steel Beam with Triangular Web Opening (SBTWO)

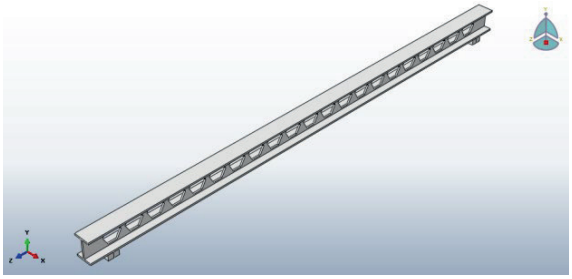

c) Steel Beam with Hexagonal Web Opening (SBHWO)

Figure 12. Representation of other steel beams modelled in Abaqus

V. RESULTS AND DISCUSSION

As it was mentioned previously the analysis concerns around the effect of the shape of the openings on the flexural behavior of the steel beams. Fig. 13 shows the applied load and mid-span deflection curve for the different types of the openings considered in the investigation.

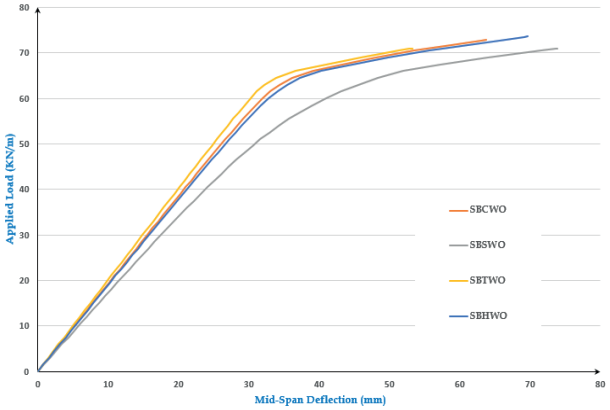

Figure 13. Comparison of load-deflection curves between different types of opening shape

By seeing the load-deflection curves shown in Fig. 13, it can be see that the stiffness of the steel beams with triangular and square web opening are greater and smaller than the stiffness of the other shapes, respectively. For all beams the plastic range of the curves starts from almost (30 mm) mid-span deflection at this point the amount of the applied load on the steel beams are (59.42 KN/m), (56.77KN/m), (55.68 KN/m) and (49 KN/m), for (SBTWO), (SBCWO), (SBHWO) and (SBSWO), respectively. Though, despite of the maximum load carrying capacities and maximum deflections are not in the same order, but in this study it was assumed that any strength of a beam after a mid-span deflection more than (30 mm) (almost after elastic range) is not considered safe strength since the deflection would be so large that it can be considered as failed beam. Thus, in this investigation the steel beam with triangular web opening considered to have the best performance in flexural resistance under the applied load. However, the maximum load carrying capacity and corresponding

maximum mid span deflection for every tested beam in this analysis is illustrated in Table 3.

Table 3. FEM Test Results

No.	*Beam Symbol*	*W (KN/m) at Δ = 30 mm*	*W_{max} (KN/m)*	*$Δ_{max}$ (mm)*
1	SBCWO	56.77	72.9	63.82
2	SBSWO	49	70.92	73.89
3	SBTWO	59.42	70.98	53.3
4	SBHWO	55.68	73.61	69.73

VI. SPECIMENS STRESS DISTRIBUTION AND DEFORMED SHAPE

The following figures, Fig.14, illustrates the stress distribution and deformed shape of the analytically tested samples with different types of web openings by subjecting the distributed load on samples top surface in F.E. analysis models.

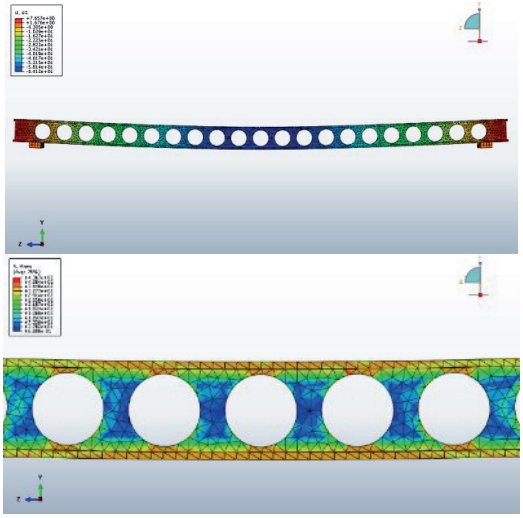

a) The deformed shape and stress distribution for FEM tested specimen (SBCWO)

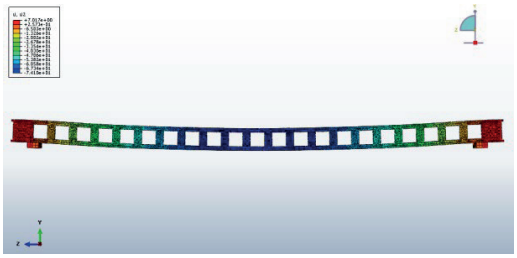

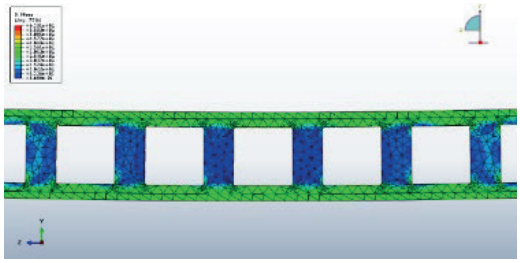

b) The deformed shape and stress distribution for FEM tested specimen (SBSWO).

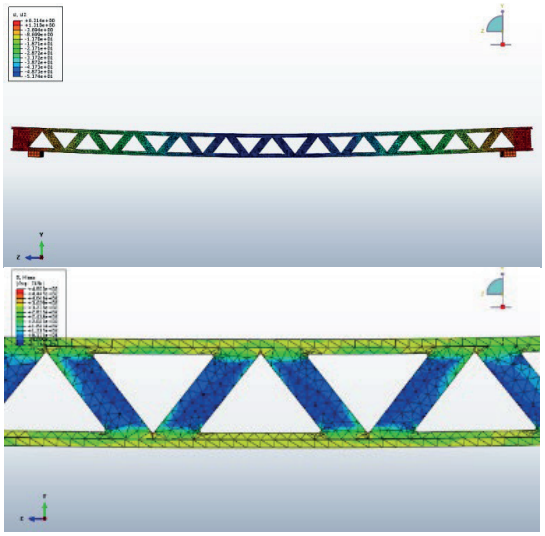

c) The deformed shape and stress distribution for FEM tested specimen (SBTWO)

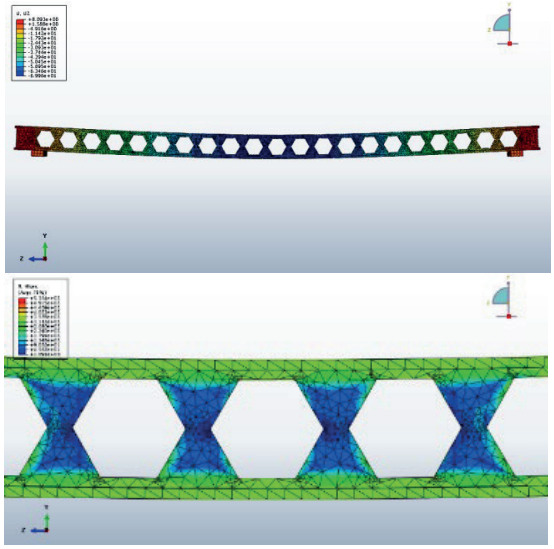

d) The deformed shape and stress distribution for FEM tested specimen (SBHWO)

Figure 14. The deformed shape and stress distribution of the tested steel beams with web openings

Form the figure above it can be observed that the stress distribution will be more concentrated at the regions between the openings and it reduces by increasing the width of this region.

VII. CONCLUSIONS

The chief aim of this work was to examine the flexural behavior of steel beam with different types of opening in the web by using a nonlinear simulation software (Abaqus). Thus, some model tests are established on SBWOs. The subsequent results and conclusions are complete in accordance of the obtained simulated SBWO models test results:

1) Test results of the analysis demonstrations that the load carrying capacity and the stiffness of the steel beam with triangular web opening is greater than the other three shapes which are circular, square and hexagonal at the elastic region by (4.66%, 21.26%, 6.71%) respectively.

2) The ultimate load at which the specimen fails will causes very large amount of deflection, thus the applied load which causes 30 mm deflection was the control value of the comparisons.

3) The circular web opening shows almost similar response to flexural stress as the hexagonal opening, this may be due to the shape of the hexagonal geometry which has more internal angles and make it to be more like a circle shape.

4) Furthermore, the square web opening has the least strength and stiffness due to large flexural stress concentration around its corners. Also, the deformations in the rectangular opening sample is greater than other test samples.

REFERENCES

1. **Samadhan G**. Morkhade1, and Laxmikant M. Gupta1 (2015), *"An experimental and parametric study on steel beams with web openings"*, Int J Adv Struct Eng, Vol. 7, P.P. 249–260.
2. **Bower J.E.** (1968), *"Design of beam with web openings"*, J Struct Div 94, Vol. 3, P.P.783–807.
3. **Lawson R.M.** (1987), *"Design for openings in the webs of composite beams"*, CIRIA Special Publication and SCI Publication 068. CIRIA/Steel Construction Institute, London.
4. **Darwin D.** (1990), *"Steel and composite beams with web openings"*, Steel design guide series no. 2. AISC, Chicago.
5. Design of composite beams with large web openings. SCI P355 (2011).
6. **Redwood R.G.** (1969), *"The strength of steel beams with unreinforced web holes"*, Civil Eng. Public Works Rev 64(755): P.P.559–562
7. **Chan P.W., Redwood R.G.** (1974), *"Stresses in beams with circular eccentric web holes"*, J Struct Div 100(ST1): P.P.231–248
8. **Olander H.C.** (1953), *"A method of calculating stress in rigid frame corners"*, J Struct Div Proc. ASCE
9. **Sahmel P.** (1969), *"Konstruktive Ausbildung und Näherungsbenechaung geschewisster Biegeträger und Torsionsst äbe mit grossen stegausnehmungen"* [The design, construction and approximate analysis of weld beams and torsion members having large web openings]. Schweissen und Schneiden 21(3): P.P.116–122
10. European committee for standardization. EN 1993-1-3, Euro code 3 (EC3) (1998) Design of steel structures—part 1.1: general rules and rules for buildings; 1992, and amendment A2 of Euro code 3: Annex N ‘Openings in webs’. British Standards Institution.
11. **Thevendran V., Shanmugam N.E.** (1991), *"Lateral buckling of doublysymmetric beams containing openings"*, J Eng Mech 117(7): P.P.1427–1441
12. **Lawson R.M., Chung K.F.** (2001), *"Simplified design of composite beamswith large web openings to Euro code 4",* J Constr Steel Res 57: P.P.135–163

13. **Chung K.F., Liu T.C.H., Ko A.C.H.** (2001), *"Investigation on Vierendeelmechanism in steel beams with circular web openings"*, J Constr Steel Res 57: P.P. 467–490
14. **Chung K.F., Liu T.C.H., Ko A.C.H.** (2003), *"Steel beams with large webopenings of various shapes and sizes: an empirical designmethod using a generalized moment–shear interaction curve",*J Constr Steel Res 59: P.P.1177–1200
15. **Tsavdaridis K.D., D'Mello C.** (2011), *"Web buckling study of thebehaviour and strength of perforated steel beams withdifferent novel web opening shapes"*, J Constr Steel Res 67: P.P.1605–1620
16. **Sweedan A.M.I.** (2011),*"Elastic lateral stability of I-shaped cellular steel beams",* J Constr Steel Res 67: P.P.151–163
17. **Saka M.P., Erdal F**. (2013),*"Ultimate load carrying capacity of optimally designed steel cellular beams"*, J Constr Steel Res 80: P.P.355–368
18. **Panedpojaman P., Thepchatri T.** (2013), *"Finite element investigation ondeflection of cellular beams with various configuration"*, Int JSteel Struct 13: P.P.487–494
19. **Boissonnade N., Nseir J., Lo M., Somja H.** (2014), *"Design of cellularbeams against lateral torsional buckling",* Proc Inst Civil EngStruct Build 167:436–444
20. **Iman Satyarno, Djoko Sulistyo, Dina Heldita, A.** Talodaci Corte Real De Oliviera (2017), *"Full height rectangular opening castellated steel beam partially encased in reinforced mortar"*, Procedia Engineering 171: P.P. 176 – 184
21. **Made Sukrawa** (2017), *"Finite element modelling of reinforced large-opening on the web of steel beam considering axial forces"*, AIP Conference Proceedings 1903, 020018, P.P. 1-9
22. **Tarek Almusallam, Yousef Al Salloum, Hussein Elsanadedy, Abdulhafiz Alshenawy and Rizwan Iqbal** (2018), *"Behavior of FRP-Strengthened RC Beams with Large Rectangular Web Openings in Flexure Zones: Experimental and Numerical Study"*, Int J Concr Struct Mater 12:47, P.P. 1-28
23. **Morkhade, S.G., Baswaraj, S.M. & Nayak, C.B.** (2019), *"Comparative study of effect of web opening on the strength capacities of steel beam with trapezoidally corrugated web"*, Asian J Civ Eng 20, P.P.1089-1099
24. BS 5950: Part 1 (2000),*"Structural use of steelwork in building"*, BritishStandards Institution, London: Code of practice for design.Rolled and welded sections
25. Abaqus (6.14-4), *"Analysis User's Manual"*, U.S.A. (2014).
26. **Mohammad R.K.M. Al-badkubi** (2019), *"Finite Element Study on Ultimate Shear Capacity of Voided Reinforced Concrete Beams"*, 2nd International Conference on Engineering Technology and their Applications 2019-IICET2019- Islamic University, Alnajaf-Iraq, P.P. 19-24

СПИСОК ЛИТЕРАТУРЫ

1. **Samadhan G**. Morkhade1, and Laxmikant M. Gupta1 (2015), *"An experimental and parametric study on steel beams with web openings"*, Int J Adv Struct Eng, Vol. 7, P.P. 249–260.
2. **Bower J.E.** (1968), *"Design of beam with web openings"*, J Struct Div 94, Vol. 3, P.P.783–807.
3. **Lawson R.M.** (1987), *"Design for openings in the webs of composite beams"*, CIRIA Special Publication and SCI Publication 068. CIRIA/Steel Construction Institute, London.
4. **Darwin D.** (1990), *"Steel and composite beams with web openings"*, Steel design guide series no. 2. AISC, Chicago.
5. Design of composite beams with large web openings. SCI P355 (2011).

6. **Redwood R.G.** (1969), *"The strength of steel beams with unreinforced web holes"*, Civil Eng. Public Works Rev 64(755): P.P.559–562
7. **Chan P.W., Redwood R.G.** (1974), *"Stresses in beams with circular eccentric web holes"*, J Struct Div 100(ST1): P.P.231–248
8. **Olander H.C.** (1953), *"A method of calculating stress in rigid frame corners"*, J Struct Div Proc. ASCE
9. **Sahmel P.** (1969), *"Konstruktive Ausbildung und Näherungsbenechaung geschewisster Biegeträger und Torsionsst äbe mit grossen stegausnehmungen"* [The design, construction and approximate analysis of weld beams and torsion members having large web openings]. Schweissen und Schneiden 21(3): P.P.116–122
10. European committee for standardization. EN 1993-1-3, Euro code 3 (EC3) (1998) Design of steel structures—part 1.1: general rules and rules for buildings; 1992, and amendment A2 of Euro code 3: Annex N 'Openings in webs'. British Standards Institution.
11. **Thevendran V., Shanmugam N.E.** (1991), *"Lateral buckling of doublysymmetric beams containing openings"*, J Eng Mech 117(7): P.P.1427–1441
12. **Lawson R.M., Chung K.F.** (2001), *"Simplified design of composite beamswith large web openings to Euro code 4",* J Constr Steel Res 57: P.P.135–163
13. **Chung K.F., Liu T.C.H., Ko A.C.H.** (2001), *"Investigation on Vierendeelmechanism in steel beams with circular web openings"*, J Constr Steel Res 57: P.P. 467–490
14. **Chung K.F., Liu T.C.H., Ko A.C.H.** (2003), *"Steel beams with large webopenings of various shapes and sizes: an empirical designmethod using a generalized moment–shear interaction curve",*J Constr Steel Res 59: P.P.1177–1200
15. **Tsavdaridis K.D., D'Mello C.** (2011), *"Web buckling study of thebehaviour and strength of perforated steel beams withdifferent novel web opening shapes"*, J Constr Steel Res 67: P.P.1605–1620
16. **Sweedan A.M.I.** (2011),*"Elastic lateral stability of I-shaped cellular steel beams",* J Constr Steel Res 67: P.P.151–163
17. **Saka M.P., Erdal F**. (2013),*"Ultimate load carrying capacity of optimally designed steel cellular beams"*, J Constr Steel Res 80: P.P.355–368
18. **Panedpojaman P., Thepchatri T.** (2013), *"Finite element investigation ondeflection of cellular beams with various configuration"*, Int JSteel Struct 13: P.P.487–494
19. **Boissonnade N., Nseir J., Lo M., Somja H.** (2014), *"Design of cellularbeams against lateral torsional buckling",* Proc Inst Civil EngStruct Build 167:436–444
20. **Iman Satyarno, Djoko Sulistyo, Dina Heldita, A.** Talodaci Corte Real De Oliviera (2017), *"Full height rectangular opening castellated steel beam partially encased in reinforced mortar"*, Procedia Engineering 171: P.P. 176 – 184
21. **Made Sukrawa** (2017), *"Finite element modelling of reinforced large-opening on the web of steel beam considering axial forces"*, AIP Conference Proceedings 1903, 020018, P.P. 1-9
22. **Tarek Almusallam, Yousef Al Salloum, Hussein Elsanadedy, Abdulhafiz Alshenawy and Rizwan Iqbal** (2018), *"Behavior of FRP-Strengthened RC Beams with Large Rectangular Web Openings in Flexure Zones: Experimental and Numerical Study"*, Int J Concr Struct Mater 12:47, P.P. 1-28
23. **Morkhade, S.G., Baswaraj, S.M. & Nayak, C.B.** (2019), *"Comparative study of effect of web opening on the strength capacities of steel beam with trapezoidally corrugated web"*, Asian J Civ Eng 20, P.P.1089-1099

24. BS 5950: Part 1 (2000),*"Structural use of steelwork in building"*, BritishStandards Institution, London: Code of practice for design.Rolled and welded sections
25. Abaqus (6.14-4), *"Analysis User's Manual"*, U.S.A. (2014).
26. **Mohammad R.K.M. Al-badkubi** (2019), *"Finite Element Study on Ultimate Shear Capacity of Voided Reinforced Concrete Beams"*, 2nd International Conference on Engineering Technology and their Applications 2019-IICET2019- Islamic University, Alnajaf-Iraq, P.P. 19-24

Hussein Talab Nhabih, Department of Civil Engineering, Faculty of Engineering, Babylon University, Babylon, Iraq. E-mail: eng.hussein.t@uobabylon.edu.iq

Mohammad R.K.M. Al-Badkubi, Department of building and construction technology, Islamic University,Najaf, Iraq. E-mail: Mohammad.R.Albadkub@iunajaf.edu.iq

Marwa Marza Salman, Department of Ceramic and Building Material, Faculty of Materials Engineering, Babylon University, Babylon, Iraq. E-mail: mat.marwa.marza@uobabylon.edu.iq

Хусейн Талаб Набих, кафедра гражданского строительства, инженерный факультет, Вавилонский университет, Вавилон, Ирак. Эл. почта: eng.hussein.t@uobabylon.edu.iq

Мохаммад Р.К.М. Аль-Бадкуби, кафедра строительства и строительных технологий, Исламский университет, Наджаф, Ирак. Эл. почта: Mohammad.R.Albadkub@iunajaf.edu.iq

Марва Марза Салман, кафедра керамики и строительных материалов, факультет материаловедения, Вавилонский университет, Вавилон, Ирак. Эл. почта: mat.marwa.marza@uobabylon.edu.iq